

THESIS

PERSISTENT HOMOLOGY OF THE LOGISTIC MAP:

AN EXPLORATION OF CHAOS

Submitted by

Rachel Neville

Department of Mathematics

In partial fulfillment of the requirements

For the Degree of Master of Science

Colorado State University

Fort Collins, Colorado

Spring 2014

Master's Committee:

Advisor: Patrick Shipman

Chris Peterson
Stephen Thompson

Copyright by Rachel Neville 2014

All Rights Reserved

ABSTRACT

PERSISTENT HOMOLOGY OF THE LOGISTIC MAP:

AN EXPLORATION OF CHAOS

Given a discrete sampling of points, how can one reconstruct the underlying geometric object? Further, the question arises how can one discern between noise and sampling distortion and important topological features. Algebraic and topological techniques used computationally can prove to be powerful and currently unconventional tools to understand the “shape” of data. In recent years, persistent homology has been explored as a computational way to capture information regarding the longevity of topological features of discrete data sets. In this project, the persistent homology of functions is explored specifically as a way of examining features of functions. Persistent homology tracks the longevity of connected components of level sets in a persistence diagram. By connecting points generated by a discrete time dynamical system with line segments, this data can be viewed as a (piece-wise linear) function, persistent homology is used to track features of the data. This provides a novel and useful tool for computationally examining dynamical systems.

The logistic map is one of the simplest examples of a nonlinear map that displays periodic behavior for some parameter values, but for others, displays chaotic behavior. When the persistence diagram is generated for an orbit of the logistic map, all of the points surprisingly lie approximately on a line. This is not true for a general sequence. This pattern arises not only after stability has been reached in the periodic case, but also as points approach stability for parameters in the periodic regime but also perhaps more surprisingly, for parameter values that lie in the chaotic regime as well. In fact, the slope of this line is fairly similar as the

parameter values are varied. This arises from the order in which the points pair to form the persistence diagram and a scaling factor seen in the periodic regime of a class of maps (including the logistic map). It is interesting that the effects of this scaling are still seen in the chaotic regime. This pattern not only arises for the logistic map, but for other unimodal maps and other higher dimensional systems that are “close” to these maps such as the Lorenz system.

ACKNOWLEDGEMENTS

I would like to thank Patrick Shipman for his continual enthusiasm and encouragement through this project, and for his innovative ideas and active support of exploration and discovery of unconventional mathematics. I would also like to thank my friends and family for their support. This thesis is typeset in L^AT_EX using a document class designed by Leif Anderson and modified by Matthew Niemerg.

TABLE OF CONTENTS

ABSTRACT	iii
ACKNOWLEDGEMENTS	iv
LIST OF TABLES	vi
LIST OF FIGURES	vii
Chapter 1. Introduction	1
1.1. Persistent Homology	2
1.2. Discrete-Time Dynamical Systems	12
1.3. The Logistic Map	14
Chapter 2. Persistent Homology of the Logistic Map	22
2.1. Observations	24
2.2. Periodic Regime	24
2.3. Chaotic Regime	29
2.4. Random or Stochastic r values	32
Chapter 3. Where is this Pattern Coming From?	33
3.1. Feigenbaum's Scaling Constant	33
3.2. Other Maps	43
3.3. Generalization	47
3.4. Extending to Higher Dimensions	49
Chapter 4. Conclusions	53
BIBLIOGRAPHY	55

LIST OF TABLES

1.1 The first three Betti numbers for the filtration in Figure 1.8.	9
1.2 Period doubling cascade	18
3.1 Parameters for α	35

LIST OF FIGURES

1.1 Portion of La Parade by Seurat	2
1.2 Loops on a geometric object	3
1.3 Data points of underlying object	4
1.4 Example and non-example of a simplicial complex	5
1.5 Sample simplicial complex	5
1.6 Effect of boundary operator	6
1.7 Three simplicial complexes with different ϵ	8
1.8 Filtration of simplicial complexes	9
1.9 Making the persistence diagram of a function	10
1.10 Cobweb diagram with fixed point	13
1.11 Cobwebbing of the logistic map	15
1.12 Bifurcation diagram of the logistic map	16
1.13 Feigenbaum's δ	19
1.14 Chaos example	20
1.15 Lyapunov exponents of logistic map	21
2.1 Persistence diagram of logistic map	23
2.2 Order in pairing points	25
2.3 Example of a typical transient behavior	27
2.4 Stability of the slope	27

2.5	Parameter dependence of the slope	28
2.6	Actual and predicted slope, maximum	30
2.7	Actual and predicted slope comparison	31
2.8	Persistence for stochastic r	32
3.1	α on bifurcation diagram	35
3.2	α boxes on updating function	36
3.3	Schematic of a period doubling bifurcation	37
3.4	Persistence of stable 4-cycle	37
3.5	Schematic of the scaling pattern	39
3.6	Scaling and the slope	39
3.7	Bifurcation diagram with unstable orbits	41
3.8	Lyapunov exponent and slope	42
3.9	Persistence of tent map	44
3.10	Persistence of quadratic map	45
3.11	Persistence of circle map	46
3.12	Persistence of bimodal tent map	47
3.13	Persistence of the Lorenz attractor	50
3.14	Persistence of the Rössler attractor	51

CHAPTER 1

INTRODUCTION

Given a set of data, we often want to be able to understand a general “shape” of the data from a topological point of view. For example if we consider our data to be a sampling of an object in three dimensional space, we may ask how many holes does this object have? Homology provides an algebraic structure to understand this question by characterizing features of geometric object. However, when the structure of the underlying object is unknown, it is useful to consider which features continue, or persist, through dimension reductions of an ascending chain of overlaid structure. The features that “last” through more reductions are in some sense more important than ones that only appear for a short time. Persistent homology is precisely the algebraic tool that allows us to do this. When applied to discrete data sets, persistent homology gives insight into the topological structure and gives a way to distinguish between major features, minor features and noise in the data. Here lies beautiful applications of pure algebraic topology to point cloud data and beyond which has led to the recent growth of this rich field. It is in the discrete setting that we find out footing for this project. In this paper we explore what this tool can tell us about discrete dynamical systems, a direction that has not been considered extensively. Initially, we set out to find an underlying structure of Liesegang rings that appear in a classical chemistry experiment, but along the way, we found some surprising results pertaining to chaotic dynamical systems.

We begin our discussion with a brief introduction to simplicial homology to gain context and foundation for understanding persistent homology. This is offered as an introduction to persistent homology as a powerful tool in computational topology and this specific version of persistent homology motivates the computations in the project. We will then proceed to

the extension of persistent homology to functions. The “data” that is at the core of this project comes from the logistic map. An introduction to this one dimensional discrete time dynamical system is given. We then will move into the main results of this project: applying persistent homology to points in the orbit of the logistic map as the parameter is varied. A clear line appears in the persistence diagram of the logistic map. This behavior is explored in both the periodic and chaotic regime. Patterns are noted in the way that the persistence diagram forms. This allows us to see that a universal scaling constant extends beyond its original scope. It is hypothesized why this pattern is occurring, specifically in connection with this scaling constant. We conclude by noting this pattern (or its absence) in several other maps and higher dimensional chaotic systems. This gives us a way to look at the “backbone” or governing system for higher dimensional systems.

1.1. PERSISTENT HOMOLOGY

In a notice from the AMS entitled “What is...Persistent Homology?” Shmuel Weinberger made the following apt analogy to introduce this idea. Consider a painting in the style of post-impressionist painter Georges-Pierre Seurat, (Fig.1.1) composed completely of tiny colored dots. The mind of the viewer infers a continuous image from discrete points. For the brain this response is automatic, but from the perspective of data analysis this is a difficult problem, especially in higher dimensions. Given a discrete sampling of points, how can we reconstruct the underlying geometric object? Further, the question arises how can one discern between noise and sampling distortion and important topological features.



FIGURE 1.1. A small portion of *La Parade* by Seurat. The image of a man can be seen even though the image is composed completely of colored dots [1].

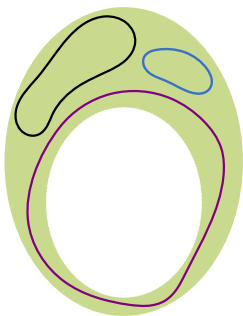


FIGURE 1.2. An object with several loops on its surface.

From a classic topological perspective, considering the equivalence classes of associated homotopy groups, that is, paths or loops along the surface of the object that can be continuously deformed into one another is an effective method for distinguishing between topological objects. In Figure 1.2 the black loop and blue loop can be continuously stretched, bent squeezed and wiggled into each other while remaining on the surface of the object. We can think of them as being in the same equivalence class. (That is they capture the same information about the object.) The purple loop cannot be stretched, bent or wiggled to match the shape of the other two loops without breaking because of the hole in the center of the loop. This loop is then taken to be in a different equivalence class. These are in fact the only two classes of loops. The two equivalent loops give us the idea that there is a hole in our object. Considering equivalence classes of loops and their higher dimensional version is the rough idea of homotopy groups [2]. However, in higher dimensions this becomes become extremely computationally expensive if not impossible to compute [3]. Another computable invariant is homology groups, which are computationally much more friendly than homotopy groups, though intuitively not quite as transparent. Roughly speaking, the equivalence relation on loops is extended: two loops are considered equivalent if there is a surface whose boundary is equal to the union of these two loops [2]. In this section, we will focus on simplicial homology; a restriction of the general theory of homology, known as singular homology. Most of the time, and especially in low dimensions, simplicial and singular homology are equivalent.

1.1.1. A QUICK INTRODUCTION TO SIMPLICIAL HOMOLOGY.

In this setting, we are after a way to characterize connected components, holes and higher dimensional voids of point cloud data, but to get a computational handle on our object we will need to discretize our space and give it some structure. Instead of looking at deforming paths into each other, we will look at interesting boundary cycles of the structure we put on the data. We will assume some basic notions of algebra, but will take a moment to establish a few of the more technical building blocks of simplicial complexes. A $(k + 1)$ -tuple of points (x_0, x_1, \dots, x_k) in \mathbb{R}^n is **affinely independent** if the set of vectors given by $\{x_0 - x_j | 1 \leq j \leq k\}$ is linearly independent. A p -**simplex** σ is the **convex hull** of $p+1$ affinely independent points and is denoted $\sigma = \text{conv}\{x_0, \dots, x_p\}$. The convex hull is the solid polyhedron determined by the $p + 1$ vertices. For example, a 0-simplex is a vertex, a 1-simplex is an edge, a 2-simplex is a triangle and a 3-simplex is a tetrahedron [4, 5].

A **face** of a simplex is a the convex hull of the set of points forming the simplex, minus one. For example, the faces of a triangle are each of the three edges and the face of an edge is the set of two vertices that were connected to create that edge.

A **simplicial complex** K is a finite collection of simplices where any face of a simplex is then itself a simplex in K . Further the intersection of any two simplices in K is either empty or a face of both simplices. For example, in Figure 1.4 the object on the left is a simplicial complex because the face of every simplex is included and when simplices non-trivially intersect, their intersection is included in the complex and is itself a face of the two

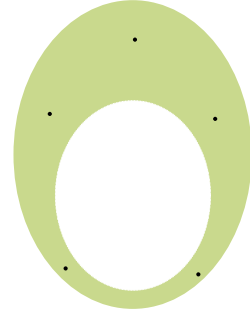


FIGURE 1.3. We begin by considering a very simple example. The green shows the underlying object and the five points show the data points we are given to attempt to reconstruct the basic features of the data.

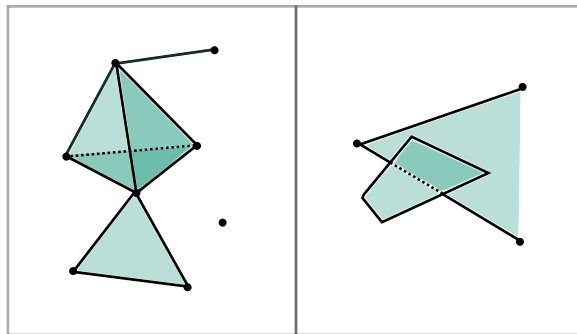


FIGURE 1.4. The figure on the left is a simplicial complex, the one on the right is not.

intersected simplices. However, in the complex on the right, the face of the triangle is not included in the complex, a quadrilateral is not the convex hull of four points, a tetrahedron is. The quadrilateral does not even include its vertices. It intersects the triangle on one of its edges, but this is not a face of the triangle. If we go back to the green object (Figure 1.3), we can build a simplicial complex with these five vertices as shown (Figure 1.5). This simplicial complex is far from unique, but this will be discussed at length later.

A **p -chain** is a subset of p -simplices in a simplicial complex. p -chains can also be thought of as formal sums, $c = \sum r_i \sigma_i$ where r_i is in $\mathbb{Z}/2\mathbb{Z}$, σ is a p -simplex in K . For example if our simplicial complex is a tetrahedron, each of the four triangle faces are 2-simplices. a 2-chain is any subset of these triangles. Similarly subsets of the edges and vertices form 1-chains and 0-chains respectively.

The set of p -chains of a simplicial complex form a p -chain group, called C_p . It should be noted that when adding p -chains, the duplicate p -simplices cancel out. If we think in terms of formal sums, our coefficients are in $\mathbb{Z}/2\mathbb{Z}$.

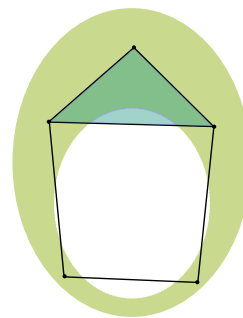


FIGURE 1.5. One of the possible simplicial complexes formed using these data points.

The **boundary** of a p -simplex is the set of $(p - 1)$ -simplices' faces and can be thought of as a formal sum of $(p - 1)$ -simplices in the simplicial complex. For example the boundary of the tetrahedron is the four triangle faces. The boundary of a p -chain is the sum of the boundaries of its simplices modulo 2. That is, faces shared by an even number of p -simplices will cancel out. Taking the boundary of a simplicial complex is a group homomorphism δ_p from C_p to C_{p-1} . In 3-dimensional space, this gives us a mapping like this:

$$\cdots \rightarrow \emptyset \rightarrow C_3 \xrightarrow{\delta_3} C_2 \xrightarrow{\delta_2} C_1 \xrightarrow{\delta_1} C_0 \xrightarrow{\delta_0} \emptyset$$

A p -chain with an empty boundary is called a p -cycle, and is the identity in C_{p-1} . The p -chains form a subspace Z_p of C_p . Z_p is by definition the kernel of δ_p . The p -chains that form the boundary of $(p + 1)$ -chains, are called p -boundary-cycles. These p -chains form B_p , a subspace of C_p , and $B_p \subset Z_p$. B_p is by definition the image of the $(p + 1)$ -boundary map. Following a diagram in [6] this can be visualized like this:

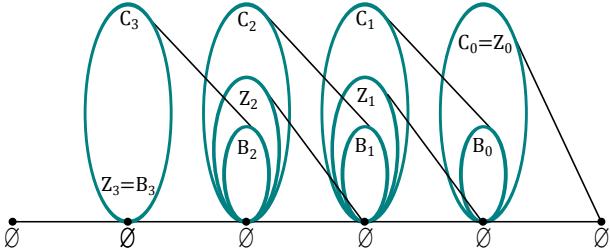


FIGURE 1.6. Schematically, the images of chain, cycle and boundary groups under the boundary operator.

The **p -th simplicial homology group** of K is the quotient group $H_p = Z_p/B_p = \ker(\delta_p)/\text{Im}(\delta_{p+1})$. The **p -th Betti number** β_p is the rank of H_p and is intuitively the number of p -dimensional holes in our object.

It should be noted that if we impose a partial ordering on the vertices, many of these computations can be done with matrices, exploiting the utility of linear algebra, but this is outside of the scope of our discussion. See [7] for more information.

1.1.1.1. *Building a Simplicial Complex.* To apply the above tool to a set of data, we need to form a simplicial complex. This becomes a combinatorial problem, because a simplicial complex formed from a set of discrete data points is far from unique. Persistent homology provides a useful tool to determine which reasonable complexes for understanding the underlying structure.

There are several different methods for building a simplicial complex from discrete data that are commonly used. We will consider the Rips complex with parameter ϵ . Each set of k points within ϵ of each other form a $(k-1)$ -simplex. For example, if two points are within ϵ of each other, they form an edge, and three points will form a triangle. This gives a simplicial complex, but the simplicial complex obviously depends on ϵ . Now incrementally increase ϵ . The simplicial complex created with the smaller ϵ is contained in the Rips complex formed with a larger ϵ . If we continue in this way, we create a nested sequence of simplicial complexes (that we can parameterize by the real numbers.) Shown in Figure 1.7 is the simplicial complex formed from a set of points using three different, increasing values of ϵ . There is a hole that appears in our complex in the first complex, however it does not seem to be part of the overall structure and disappears with the next choice of ϵ .

The question now becomes, which holes in our simplicial complex are really topological features of our data, and which ones appear “artificially” as a result of our choice of ϵ ? Persistent homology allows us to examine all ϵ ’s and track how the holes in the simplicial complex change as the ϵ ’s change. This is precisely the idea of **persistence**.

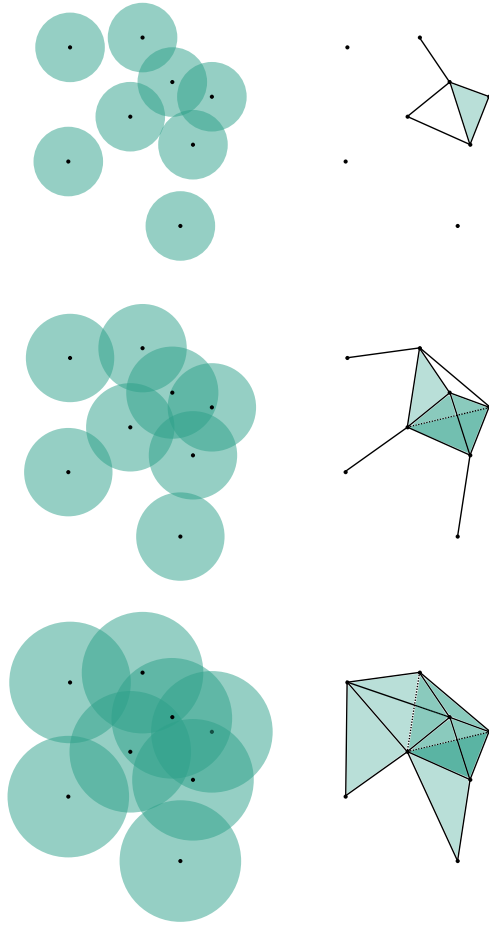


FIGURE 1.7. Three simplicial complexes formed by increasing the ϵ radius around each point.

sampled object [5].

In Figure 1.8 we can see the result of building a Rips complex from the discrete data points given in Figure 1.7. ϵ is increased to form each subsequent simplicial complex. The first three Betti numbers are tracked in Table 1.1 [7]. β_0 corresponds to the number of connected components, β_1 gives the number of 1-dimensional holes and β_2 gives the number of 2-dimensional voids.

An increasing sequence of radii $\{\epsilon_1, \epsilon_2, \dots\}$ gives rise to a sequence of increasing simplicial complexes $K_1 \subseteq K_2 \subseteq \dots$. If we start this sequence with the empty complex and end with the complete complex, this gives a **filtration**. From this ascending chain of “test” complexes, each including more connections than that of the previous one, some topological features will arise and quickly “die”, however, other topological features will last. The features that last or persist through this process provide insight into structure of the

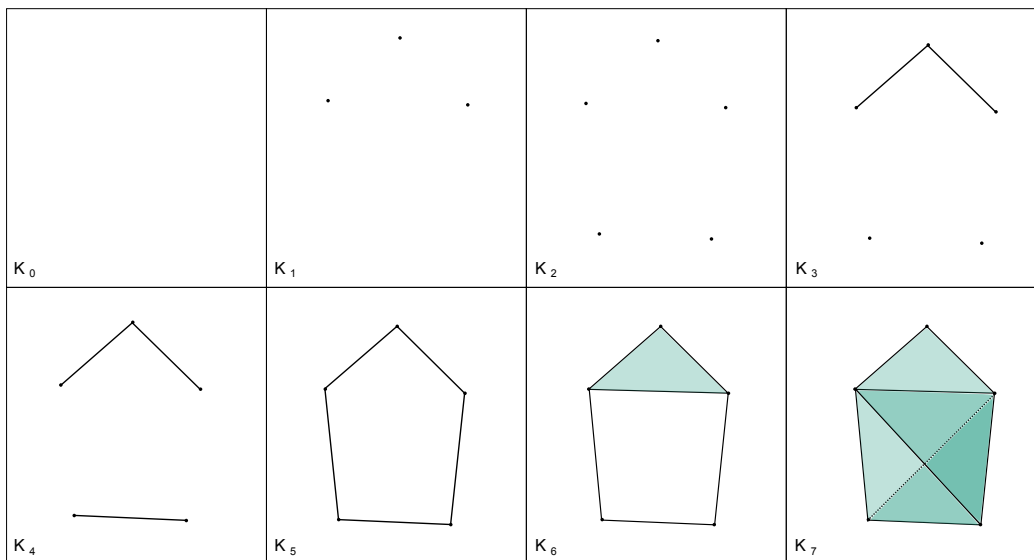


FIGURE 1.8. A filtration of simplicial complexes formed using the data points.

TABLE 1.1. The first three Betti numbers for the filtration in Figure 1.8.

Simplicial Complex	β_0	β_1	β_2
K_0	0	0	0
K_1	3	0	0
K_2	5	0	0
K_3	3	0	0
K_4	2	0	0
K_5	1	1	0
K_6	1	1	0
K_7	1	0	1

A **homology class** α is born at K_i if it is not in the image of the inclusion map from K_{i-1} to K_i . This feature then dies entering K_j if the map induced by the inclusion of $K_{i-1} \subseteq K_j$ does not include α but $K_{i-1} \subseteq K_{j-1}$ does include α . The persistence of α gives us some notion of how “long” this object existed and is given by $j - i$.

Persistent homology can also be used in the context of functions [8]. The previous information is offered only to give background on persistent homology as a tool in computational topology. In this paper, we will consider what information can be gleaned from the persistent

homology of a curve or a set of data points generated from a discrete-time series and treated as a piecewise linear function.

1.1.2. PERSISTENT HOMOLOGY OF CURVES.

We will begin with persistent homology of single variable functions. Let $f : \mathbb{R} \rightarrow \mathbb{R}$ be a smooth function with critical points when $f'(x) = 0$ with critical values $f(x)$. We will exclude points of inflection, that is, when $f''(x) = 0$ so the critical points are local minimums and maximums [7].

Let $f : \mathbb{X} \rightarrow \mathbb{R}$, where \mathbb{X} is a geometric object and f is smooth. For each $t \in \mathbb{R}$ the sublevel set $\mathbb{R}_t = f^{-1}(-\infty, t]$. In finding the persistent homology of a simplicial complex, subcomplexes of the complex are analogous to the level sets in the functional setting persistence is then the amount of “time” that this component exists through a filtration [9]. In the same way that ϵ was varied to form a filtration of nested subcomplexes, as

t varies, the level sets vary and we are given a filtration. To gain some intuition, we will use this analogy: for each $t \in \mathbb{R}$, we will think of the sublevel set $\mathbb{R}_t = f^{-1}(-\infty, t]$ as the surface of water rising under the stiff structure of the curve. The surface of the water is unbroken,

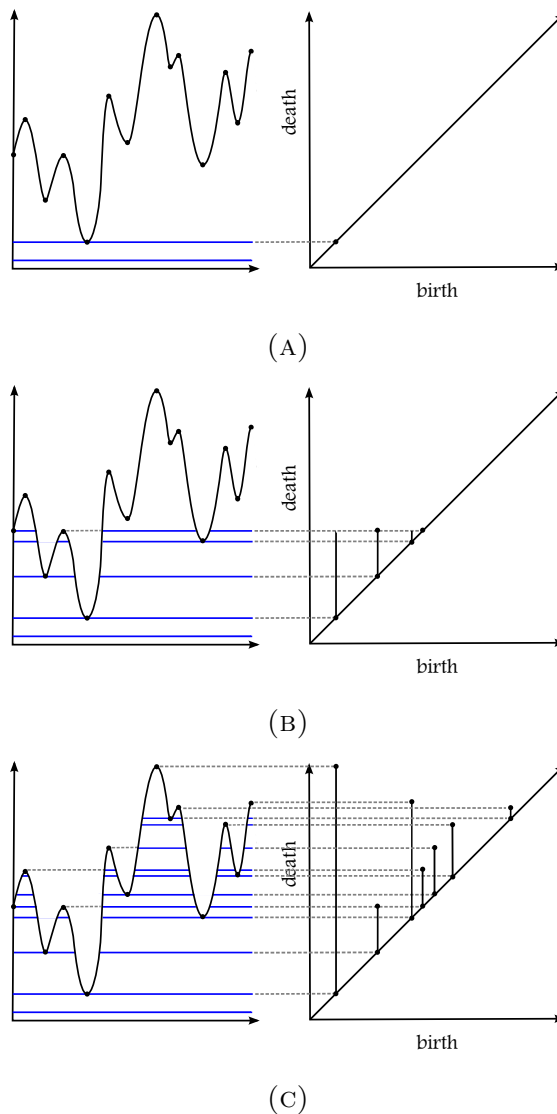


FIGURE 1.9. The making of the persistence diagram of a curve.

or is in one piece when it is completely below the graph of the function. As t increases, or the water rises, it will eventually encounter the smallest minimum value. See Figure 1.9a.

As t increases, or the water rises past this point, there are now two components of the surface of water. At each local minimum, a new component is added to the surface of the water (or more precisely, the level set). At each local minimum, a new component is formed and associated with that minimum value and this is considered the “birth” of a feature of the function. As the water rises (t increases) the number of components of \mathbb{R}_t increases incrementally as the surface of the water encounters minimums. When the surface encounters a maximum, and the surface of the water directly under this maximum disappears, (and the number of surface components decreases by one.) In fact it this maximum value marks the “death” of the component that was created by the most recent minimum. This method give us a way to track features of our function and gives us a notion of their “size.” This maximum is paired with the highest of the two minimums associated with the two components that merged at this maximum. (Commonly stated “the youngest dies first.”) It should be noted that the connectivity of the sublevel set only changes when t reaches a critical value [7, 10].

The **persistence** of the feature is defined to be the difference between the maximum value and minimum value. We are interested in which features “live” or persist the longest as they can give us topological information on our data. Persistence is easily encoded in a persistence diagram, which plots each of these persistence pairs. In this context, the persistence is often most useful when it is given by $f(y) - f(x)$ [7]. We can think of the x-axis of this diagram as the birth of new features and the y-axis as when they die. On such a diagram, the persistence is easily pictures as the vertical distance of the point from the line $y = x$. This line is called the bisectrix.

If we consider, for example, a specific sublevel set, shown above in Figure 1.9c by the top blue line, the sublevel sets has 4 components, seen by the fact that on the persistence diagram a line of this height intersects 4 bars. This is also the corresponding Betti number at this stages. Informally, the k th Betti number is the number of unconnected k -dimensional components [2]. If two spaces are homotopy equivalent, then all of their Betti numbers are the same. In this case, we are only considering the first Betti number, β_0 , which tells us the number of connected components. β_1 is the number of one-dimensional holes and does not apply to this scenario.

Finding the persistence of a function can be used in higher dimensions where the function we are considering is the distance function between points in a given measure [10]. This can give us an idea of what topological features are present in a data set. It is interesting but beyond the scope of this paper to consider the topological information that could be gathered from such an approach and the how to perhaps impose a condition on how to determine if a feature is noise or is a distinguishing feature of a data set.

1.2. DISCRETE-TIME DYNAMICAL SYSTEMS

We will focus our attention on discrete-time dynamical systems in one dimension. Let $f : \mathbb{R} \mapsto \mathbb{R}$ be a real valued function, called a map. Starting from an initial point, x_0 , f maps to the sequence $\{x_0, f(x_0), f^2(x_0), \dots, f^n(x_0) \dots\}$ where $f^n(x_0)$ represents the n th composition of f with itself. The sequence $\{x_0, f(x_0), f^2(x_0), \dots, f^n(x_0) \dots\}$ is called the **orbit** of x_0 under f . We can also write this map as $x_{n+1} = f(x_n)$ (which is often referred to as a first order difference equation).

When $f(x^*) = x^*$, x^* is called a **fixed point**. Fixed points play an important role in understanding the dynamics of the system. Sometimes a system will stabilize to a set of

fixed points after a number of iterations displaying periodic behavior. When $f^n(x_0) = x_0$, x_0 is a periodic point of period n .

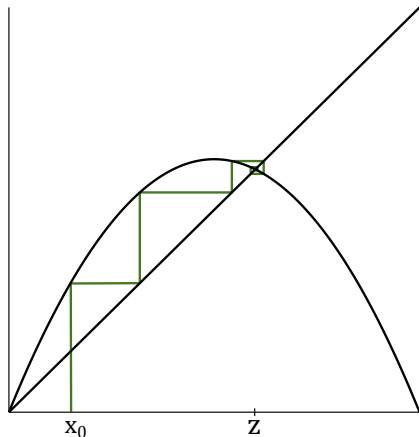


FIGURE 1.10. A cobweb diagram with a fixed point at z .

It is easy to visualize these systems through graphical iteration using a tool called cobwebbing. Begin by plotting the function $y = f(x)$ and the line $y = x$. Start at the point (x_0, x_0) on the diagonal and move vertically to the graph of f . Now we are at $(x_0, f(x_0))$ which is (x_0, x_1) . Now move horizontally back toward the diagonal, to (x_1, x_1) . Repeat this process, moving vertically

to $(x_1, f(x_1)) = (x_1, x_2)$ and horizontally back to the diagonal at (x_2, x_2) . This process visually shows the orbit of a point and gives us an intuitive understanding of long term behavior and can be seen, for example, in Figure 1.10.

The fixed point is clear in this case, starting at x_0 when x_0 is at the intersection of the diagonal and the graph of $f(x)$ will remain stationary when iterated. We can see in Figure 1.10 that the point x_0 tends towards the fixed point z . We call z an attracting fixed point for f or a sink since there is some neighborhood U of z such that if $x \in U$ then $f^n(x) \in U$ for all n and $f^n(x) \rightarrow z$ as $n \rightarrow \infty$. Formally if z is a fixed point and $|f'(z)| < 1$ then z is a sink [11]. Notice that under iterates of f , the initial point y_0 moves away from the point z . That is, for z a fixed point The point y_0 is called a source or a repelling fixed point if all orbits leave U under iteration of f . Likewise, a fixed point z can be identified as a source if

$|f'(z)| > 1$. If $|f'(z)| = 1$ then z is called indifferent or neutral and is neither attracting nor repelling [12].

Often discrete dynamical systems depend on a control parameter appearing in the equation, that is, $f(x, a)$. We will see that varying the control parameter a can have a large effect on the dynamics of the system [12].

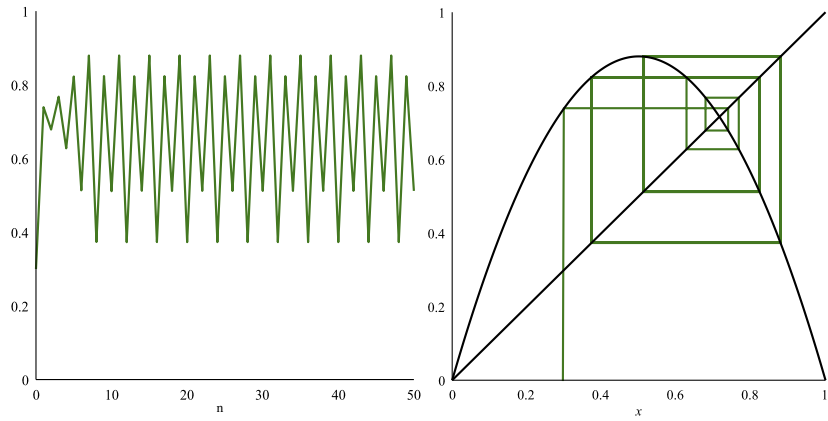
1.3. THE LOGISTIC MAP

Championed by biologist Robert May in 1976 as clear example that simple non-linear maps could have very complicated dynamics, the logistic map is one of the simplest and most well understood examples of a nonlinear discrete dynamical system and displays the most important features of low dimensional chaotic behavior. It is often used to model and understand population dynamics. The logistic map, is given by

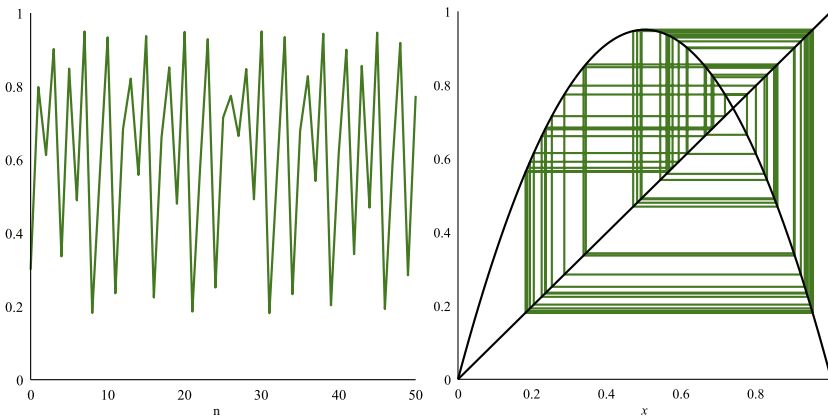
$$x_{n+1} = rx_n(1 - x_n)$$

for $0 \leq x_0 \leq 1$ and $0 \leq r \leq 4$. This provides a rich example to explore periodic regions, complex chaotic behavior and self similarity. The logistic map maps the unit interval $I = [0, 1]$ into itself for values of $r \in [0, 4]$ which means that I is forward invariant. Figure 1.11a shows behavior in the periodic regime, where after a few iterations, the system settles into a periodic 4-cycle. Figure 1.11b shows chaotic behavior. This will be more precisely defined later, but as shown here, there is not a clear repeated pattern.

It should be noted that any quadratic polynomial can be written in the form $f(x) = a - x^2$ under the correct change of variable. Changing variables does not change the qualitative dynamic behavior of the system. The introduction to the logistic map given in [11] gives a nice framework for understanding some of the structure of this map. The next section follows this introduction.



(A) Cobwebbing shows the stability of the period 4-cycle for $r = 3.52$



(B) Cobwebbing displays chaotic behavior when $r = 3.8$

FIGURE 1.11

1.3.1. BIFURCATION DIAGRAM. By focusing on long term behavior, we can see where the logistic map is periodic and where it is chaotic. In general, when there is a qualitative change in the long term behavior of the map as the control parameter is varied, we say that the system underwent a **bifurcation**. In fact, the bifurcation diagram captures the orbit of points after the system has stabilized. This is the asymptotic behavior represented as a function of the control parameter. The bifurcation diagram for the logistic map is shown in Figure 1.12. Notice from the bifurcation diagram, there are different regimes where points

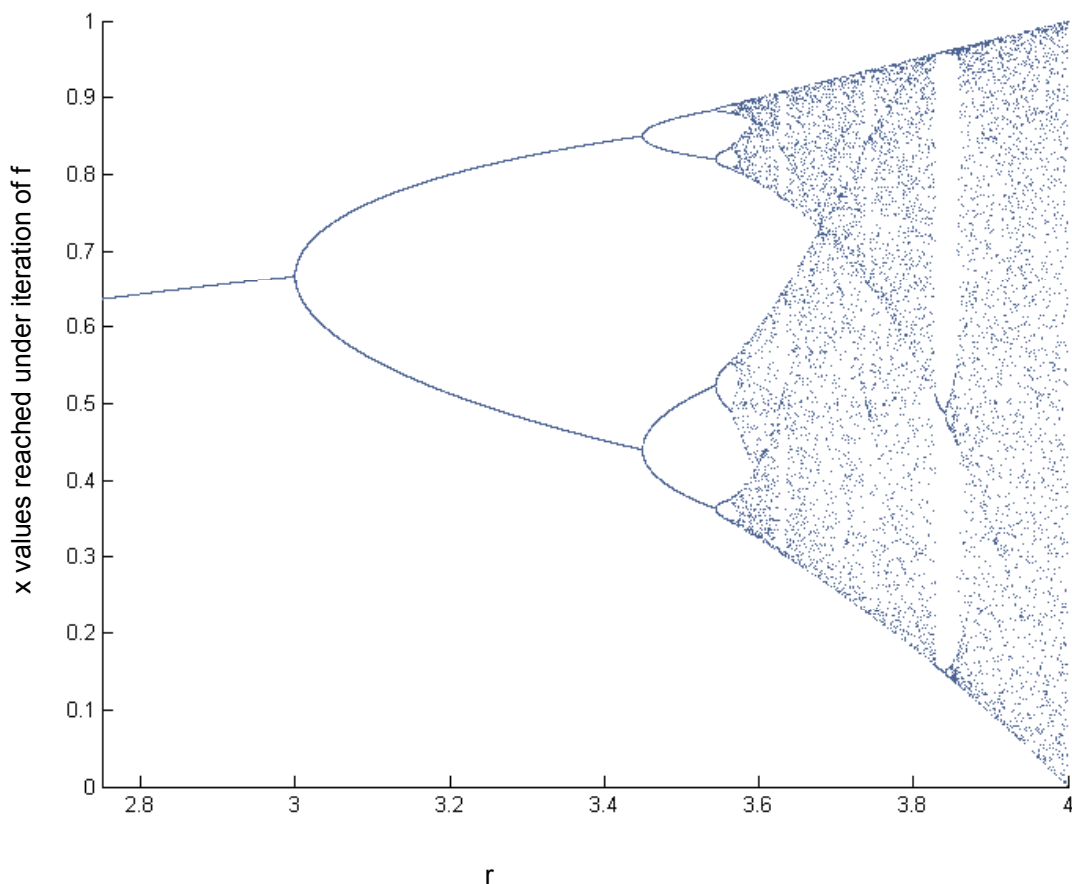


FIGURE 1.12. Bifurcation diagram of the logistic map.

behave in a certain way and parameter values at which this behavior undergoes changes. For example, for $0 < r < 3$ the system is stable and the orbit is (asymptotically) a single point.

Fixed points of this map give some insight into the dynamics of the map. The fixed points satisfy $f(x^*) = x^*$ and with a little algebra, $x^* = 0$ and $x^* = 1 - \frac{1}{r}$. This means that for all r , the origin is a fixed point $x^* = 1 - \frac{1}{r}$ is in the unit interval if $r \geq 1$. Stability is determined by $|f'(x^*)| = |r - 2rx^*|$, which means that the origin is stable for all $r < 1$ and unstable for $r > 1$. For the other fixed point to be stable, $|r - 2r(1 - \frac{1}{r})| = |2 - r| < 1$ must hold, implying that for $1 < r < 3$ this fixed point is stable and for $r > 3$ this fixed point is unstable.

At $r = 1$ we say that the fixed point at the origin splits or bifurcates in a transcritical bifurcation, that is, one fixed point will lose stability and the other will gain stability. The second fixed point (shown on the graph as x^*) remains stable as r increases until r reaches 3, at which point $f(x^*) = -1$ and the map undergoes another bifurcation called a saddle-node bifurcation. A saddle node bifurcation occurs when a single, neutral fixed point instantaneously splits into two fixed points, one attracting, or stable (called the node) and one repelling, or unstable (called the saddle).

The points that converge to an attracting fixed point are said to lie in the basin of attraction of this point. Note that the unstable fixed point that occurs on the border between the basin of attraction of the corresponding stable point and the point at infinity [13]. We notice from the bifurcation diagram (Fig. 1.12) that for $r < 3$ up until a certain point, the logistic map has a stable period 2-cycle.

To understand this better, we consider the fixed points of the second iterate of f , which can be thought of as either p and q such that $f(p) = q$ and $f(q) = p$ or the two solutions of $f^2(x) = x$. This is a quartic polynomial, which can be simplified by noting that the origin and $x^* = 1 - \frac{1}{r}$ are both solutions, (since in both cases, $f(x^*) = x^*$) and therefore $f^2(x^*) = x^*$) we factor these solutions out of the polynomial and with a little algebra find that

$$p, q = \frac{r + 1 \pm \sqrt{(r - 3)(r + 1)}}{2r}$$

. From this we can see that for $r > 3$ the solutions are real and so, for any $r > 3$ the logistic map has a 2-cycle. Now we will consider stability. The 2-cycle is stable when p and q are stable fixed points, that is, when $|\frac{d}{dx}f^2(p)| = |f'(f(p))f'(p)| = |f'(q)f'(p)| < 1$ which by symmetry is the same for q . Plugging in for p and q this simplifies to the condition

$|-r^2 + 2r + 4| < 1$ or $3 < r < 1 + \sqrt{6}$ (taking into account the domain of r). For values of $r > 1 + \sqrt{6}$ the 2-cycle is unstable, and therefore does not appear in the bifurcation diagram, however, these unstable areas play an important role in the dynamics of the map. In fact, at $r = 1 + \sqrt{6}$ there is a saddle node bifurcation to a 4-cycle [11]. It is easy to see that this bifurcation pattern will continue.

1.3.2. CHAOTIC REGIME. The logistic map displays a period doubling cascade to chaos. If we continue in the same way as above, we quickly need to rely on numerical techniques.

Denote r_n as the r value when a 2^n -cycle appears. From the bifurcation diagram we can only discern the first few locations of period-doubling, however, there are infinitely many. The sequence $\{r_n\}$ is an infinite series called a period doubling cascade, where a 2^n -cycle exist for every positive integer n . If we compute the locations of r_n numerically, we can see (in Table 1.2) that successive period doubling bifurcations occur closer and closer together. The location converges geometrically to the accumulation point $r_\infty = 3.569946\dots$. It was discovered by Feigenbaum (in 1978) that the distance between successive bifurcations shrinks by a constant factor:

TABLE 1.2. The parameter values for onset of the first several period 2^n -cycles. 1.8.

Parameter	Cycle	Value
r_1	2	3
r_2	4	3.449489728...
r_3	8	3.544090359...
r_4	16	3.5644072661...
r_5	32	3.5687594195...
r_6	64	3.5696916098...
\vdots		
r_∞		3.5699456...

$$\delta = \lim_{x \rightarrow \infty} \frac{r_n - r_{n-1}}{r_{n+1} - r_n} = 4.6692016291\dots$$

known as the Feigenbaum constant [14]. δ is a universal constant for the rate of convergence of bifurcation locations for maps approaching chaos through period doubling. This is in fact a very large class of systems.

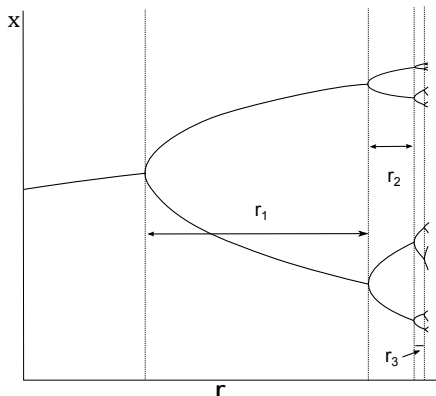


FIGURE 1.13. δ_n as shown above is the distance between r_n and r_{n+1} .

In the literature, the term “chaos” is has many different definitions, and often is used to refer to long term unpredictability of behavior in a deterministic system, referring often to a high sensitivity to initial conditions. Relying on a more technical definition, we say that a map $f : I \rightarrow I$ is chaotic if periodic points of f are dense in I , f is transitive on I , and f has a sensitivity constant

γ such that for any $x \in I$ and any open neighborhood of x there exists a $y \in I$ and $n > 0$ such that $|f^n(x) - f^n(y)| > \gamma$ [12]. We take transitive to mean that for any two subintervals U and V there exists an $x \in U$ and $n > 0$ such that $f^n(x) \in V$. It is interesting to note that the first two conditions are equivalent topological conditions while the last condition is a metric condition [11].

This occurs for parameter values greater than $r_\infty = 3.5699456\dots$ in the logistic map, though there are infinitely many periodic windows between any two periodic windows [13]. The dynamics of this map are quite complicated for $r > r_\infty$.

While a sensitive dependence on initial conditions is not sufficient for a system to be chaotic, transitivity is necessary as well [15], it is useful to consider a measure of the sensitivity to initial conditions. This is given in a **Lyapunov exponent** which measures the

exponential divergence of initial conditions that are “near” to each other. That is, if two initial conditions that are “close” to each other are iterated, soon they are no longer close to each other.

If there is an infinitesimal perturbation from an initial condition after n iterations the distance between those infinitesimally close states will grow exponentially $\delta x_n \sim e^{n\lambda} \delta x_0$ where λ is the Lyapunov

exponent. When this exponent is negative, the system is not chaotic. When this number is positive, the system is chaotic. Conceptually this can be thought of as a generalization of eigenvalues. Figure 1.15 shows a plot of the Lyapunov exponents. In the chaotic regime, small periodic windows are seen as negative exponents. (Because the parameter is varied by 0.0001, very few of the periodic orbits actually show up. More and more will appear as the increment is made smaller.)

There are a wealth of other interesting features arising when $r > r_\infty$. At $r = 1 + \sqrt{8} \approx 3.828427\dots$ there is a 3-periodic window, that undergoes a period doubling cascade to periodic behavior. This is the largest such window, and can be seen in the bifurcation diagram. Remarkably, there is a periodic window of a base k , for any odd k where the period will double to chaos [16]! Zooming in on the bifurcation diagram in any one of these regions will produce a bifurcation diagram that is itself similar to the period doubling seen in the full bifurcation diagram. These regions of self similarity provide a rich, fractal-like structure. In fact, when this map is conjugated (changing form but not the dynamics) and is considered in the complex numbers, it gives rise to the fractal pattern of the Mandelbrot set!

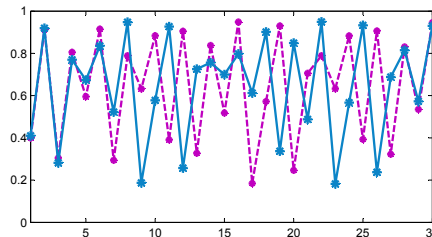


FIGURE 1.14. The initial conditions 0.4 and 0.401 iterated 30 times for the parameter value $r = 3.8$. The orbits very quickly diverge even though the initial conditions were very close.

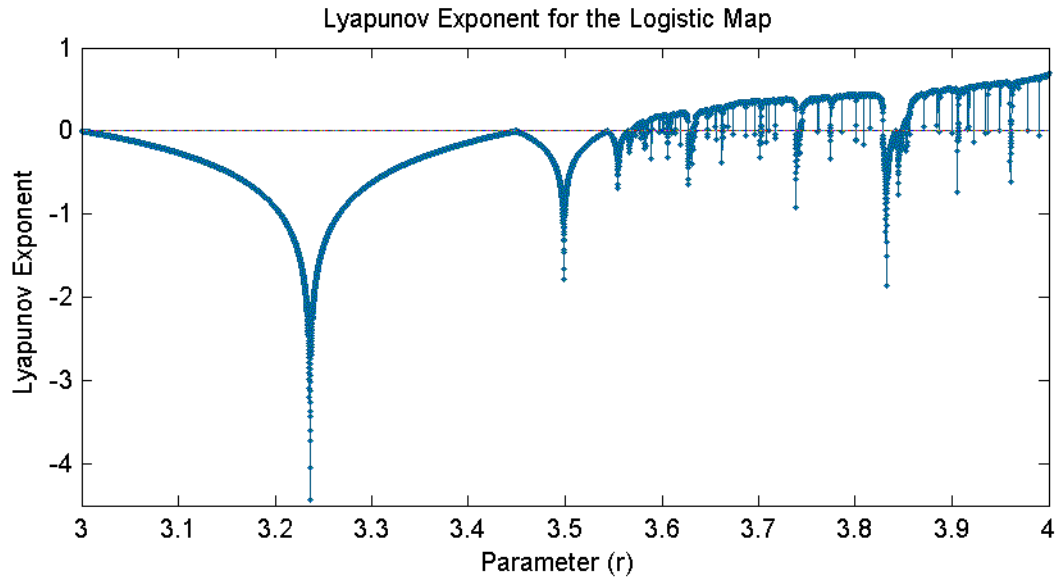


FIGURE 1.15. The Lyapunov exponents numerically computed from $r = 3$ to $r = 4$ with a step of 0.0001.

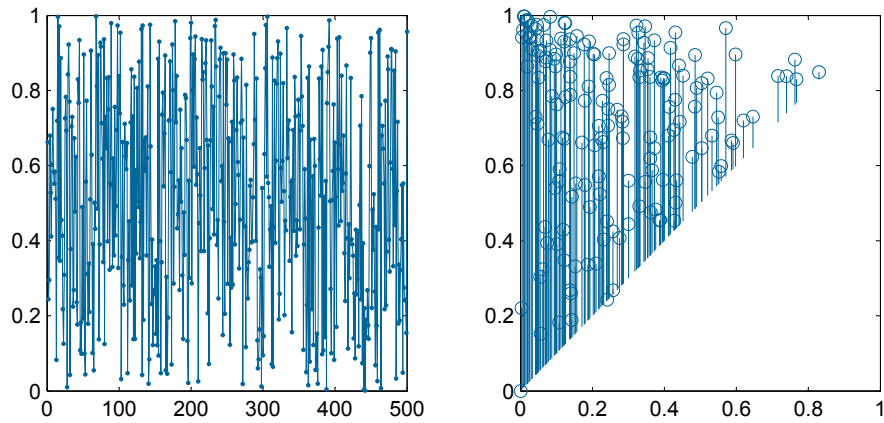
CHAPTER 2

PERSISTENT HOMOLOGY OF THE LOGISTIC MAP

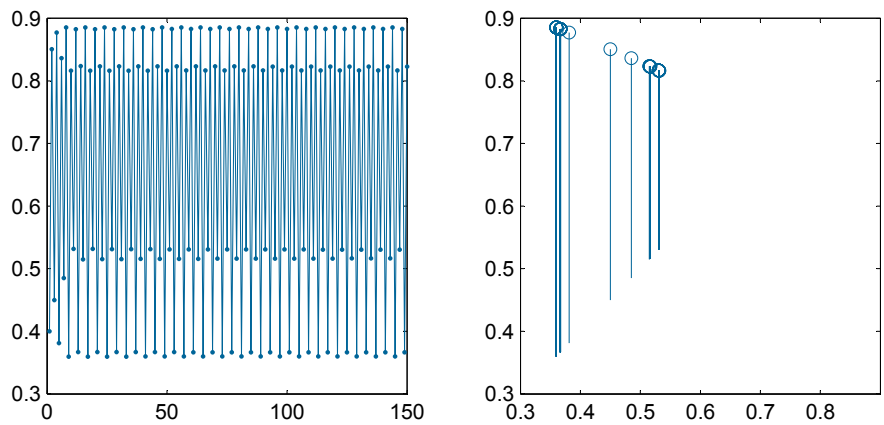
Since, from the perspective of persistent homology, all necessary information about a function is encoded in the critical values, it is possible to compute the persistent homology of the orbit of a one dimensional discrete time dynamical system. In fact, persistent homology gives a novel way to approach these systems.

When computing the persistence diagram, the only necessary information is the locations and values of relative maximums or minimums. If the points found through iteration of the logistic map are connected with line segments in the order in which they occur, a continuous (though nondifferentiable) graph is created. When thought of in this way, the points are either a local maximum, a local minimum or some an intermediate point and it is possible to calculate the persistence diagram. The orbits that happen to fall between a local maximum and a local minimum are disregarded in the calculation of the persistence diagram (as would be expected if this were a smooth function).

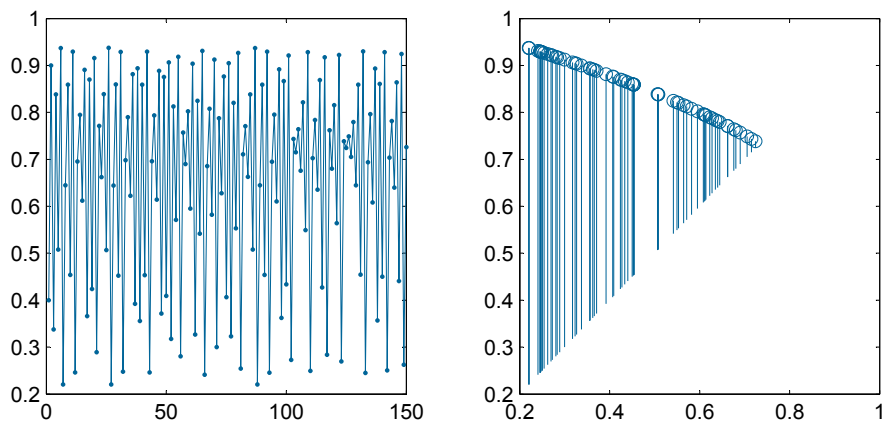
Originally, the intention of this project was to use persistent homology to better understand a Liesegang ring pattern occurring in the precipitate of the chemical reaction of gaseous NH_3 and HCl . Future investigations will be done with persistent homology of the pattern in the precipitate to better understand the dynamics of the reaction-diffusion interaction of these gases. The persistence provides a good way to classify noise in data and a novel way to compare data. However, in development of this tool, interesting patterns arose persistence diagram of the Lorenz system (to be discussed later) and the logistic map. These patterns will be discussed at length in this paper.



(A) points drawn from uniform distribution



(B) logistic map $r = 3.545$; stable 8-cycle



(C) logistic map $r = 3.75$; chaotic regime

FIGURE 2.1. In each row, the left plot is the set of discrete points (connected with line segments) that results in the given persistence diagram, right.

2.1. OBSERVATIONS

While clear patterns do not occur for a general set of points, there is a distinct pattern that appears in the persistence diagram. In fact, when points are drawn from a random (Gaussian or Normal) distribution and connected in the order in which they were drawn, there is no apparent pattern or order appearing in the associated persistence diagram. Figure 2.1a shows sampled points drawn from a Uniform distribution on the left and the persistence diagram on the right. However, when the persistence diagram is computed for the logistic map, the persistence points all fall very close to a line as seen in Figure 2.1b. Here, $r = 3.545$ which is a stable periodic 8-cycle. The four darker bars correspond to the stable periodic behavior and the other bars arise from the transient points that occur at the beginning as the system reaches stability. This is surprising! Even more interesting is the fact that this pattern is seen regardless of the initial conditions, before the orbit reaches stability, and in the chaotic regime. Figure 2.1c shows the persistence diagram for the chaotic regime, where $r = 3.75$. The persistence points lie very close to a “line” which appears to bend downward slightly into the chaotic regime. The next sections will delve further into this phenomena.

2.2. PERIODIC REGIME

We will begin with the periodic regime, first considering orbits after stability has been attained. Before the bifurcation to a stable period two cycle at $r = 3$, the system quickly stabilizes to a fixed point. Once stable this does not afford relative maximums and minimums. Even if the beginning transient points are included, there are not enough minimums and maximums to make a persistence diagram with more than one bar.

For $3 < r < 1 + \sqrt{6}$ the system stabilizes to a 2-cycle. With one minimum value and one maximum value, this affords one location for a bar in the persistence diagram. In this case,

it turns out that the line can still appear in this regime if the transient behavior is included. In these cases, it has a large effect on the slope (since there are very few points) and it does not shed much light on why this pattern arises. Through a bifurcation, each bar seems to split into two bars, one slightly higher and to the left of the original and one slightly down to the right of the original. So for a 4-cycle, there are 2 bars appearing in the persistence diagram. (The two lower points are the “births” of features and the two upper points are the “deaths”.) The bars slowly move apart on the persistence diagram as r is increased. This is expected from the bifurcation diagram and can be seen as the “tines” widening as r increases.

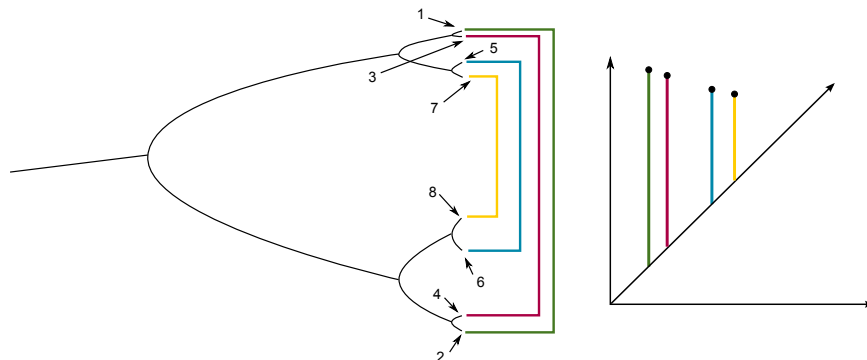


FIGURE 2.2. The brackets on the left show which minima and maxima pair with each other, the color of the bracket corresponds to the bar in the persistence diagram. This pairing is a result of how the persistence is computed, the interesting thing to note here is the order of iterations of the map.

It should be noted that the minimums and maximums pair in the same way almost every time (as illustrated in Fig. 2.2) The lowest minimum pairs with the highest maximum, then the next lowest minimum pairs with the next highest maximum, and this pattern continues. This is not surprising since it is how the persistence diagram is formed. However, if we consider the order of iteration, each maximum almost always pairs with point in the orbit that directly follows it, which is a minimum. If random points (drawn from a normal or uniform distribution) are ordered from smallest to largest and paired in a similar way,

the points generally fall so that the left most point is the highest and the rightmost point is the lowest. However, necessarily so, for if the smallest “minimum” is paired with the largest “maximum” and the largest “minimum” is paired with the smallest “maximum”, the persistence diagram will have this general feature. In this case these points very clearly do not fall in a line. There is something deeper than the order of the pairing that causes this line to appear.

There are a few occasions when points will pair in a different order. For example for the parameter value $r = 3.5$ (which produces a stable 4-cycle) and initial condition 0.715. For this initial condition, the transient behavior plays a much larger role in the formation of the persistence diagram. With these specific parameter values, there is a relatively large amount of transient behavior before the system reaches stability. See Figure 2.3. In these cases, a relative maximum will pair with the previous iteration of the map (instead of the next iteration, as is the case for most other maximums.) This appears in the persistence diagram as a second line in the persistence, to the right of the main one. The slope of this line is steeper than the pattern including the stable orbit- though it is inconsistent both in magnitude and position. Sometimes it will appear intermixed with the other line and the separation is not as drastic. Also the bars that correspond to the periodic behavior are not very clear (even after 50 iterations) because the system takes so long (compared to nearby parameters) to stabilize. If more iterations are considered, then their effect decreases until it hardly exists.

For most initial conditions, there is one major feature and the slope stabilizes fairly quickly (even when 500 iterations are used). As the orbit is settling into a periodic orbit from the initial conditions, they occur in such a way that they fall very close to the line

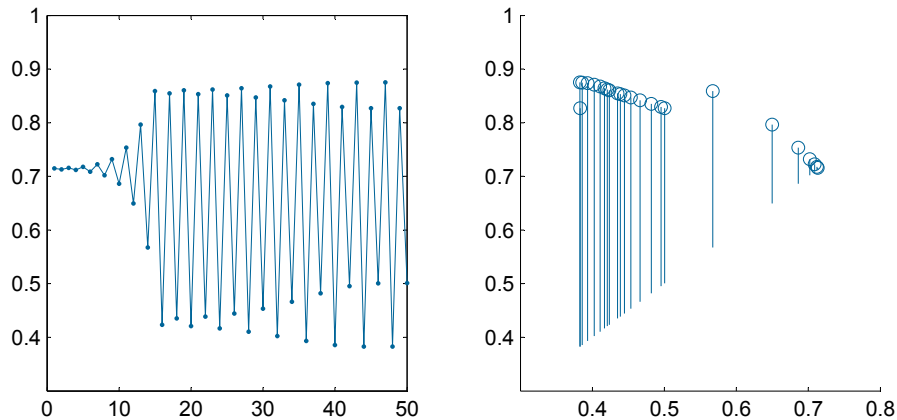


FIGURE 2.3. Shown here is an example where the transient behavior is clearly seen in the persistence diagram. The first set of persistence points is seen as a second steeper line to the right in the persistence diagram. $r = 3.5$ and the initial condition is 0.715

formed by the two persistence points. The slope of this line is consistent regardless of the initial conditions, though there are a few initial conditions for which this temporary switch in the order of pairing typically appears.

This occurs for initial conditions between 0.71 and 0.875 and is seen consistently across parameter values above the onset of the 4-cycle in the chaotic and periodic regimes. This causes an increase in the slope when calculated with a linear fit including all points, but as the number of iterations increases, their effect decreases (since there are only a finite number of points in this second formation.) There is one small blip also at 0.28 and .085 (regardless of r) for lower numbers of iterations. 0.4 appeared to be in the middle of a section where the slope stabilized very quickly and consistently regardless of r , so

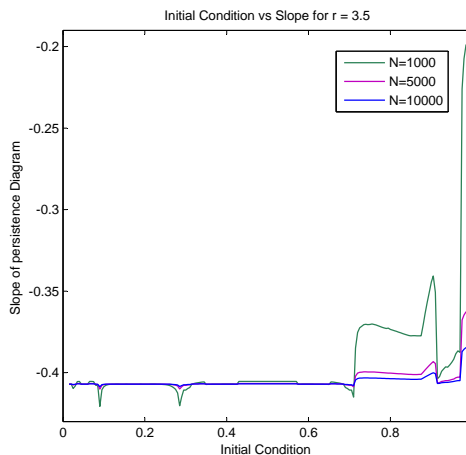


FIGURE 2.4. The stability of the slope as the number of iterations is increased

for much of the numerics, an initial condition of 0.4 was used. Also, 10,000 iterations were used so that any possible transient behavior did not have a large effect. This can be seen in Figure 2.4, where the parameter value under consideration is again 3.5.

It should also be noted that occasionally, there are a few persistence points in the region of transient behavior that do not fall on the line. It is unknown why these points appear, however it is usually one or possibly two points, so when the total number of iterations is large, their effect on the pattern is negligible.

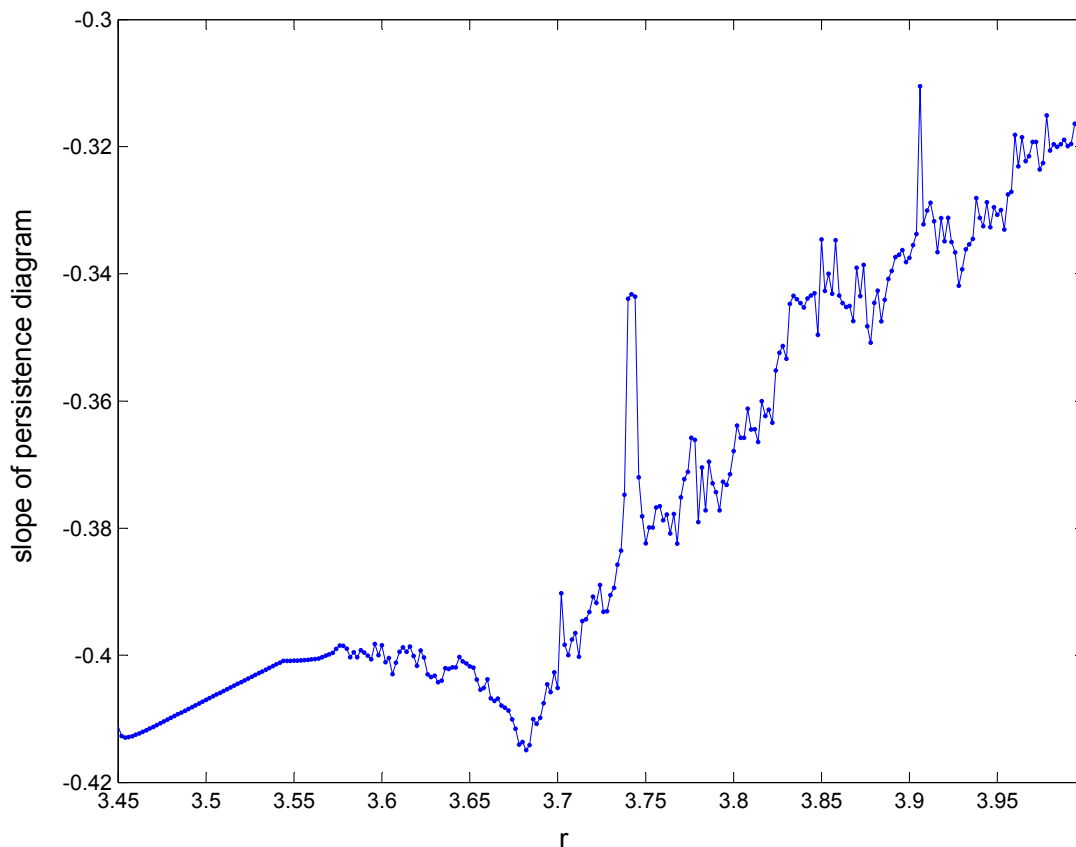


FIGURE 2.5. The r dependence of the slope of the persistence diagram. The persistence diagram was built from 10,000 iterations, with an initial condition of 0.4. r was increased by a step size of 0.001.

For large enough orbits of points, the slope is consistent across initial conditions (barring some initial transient behavior). In much of the generation of data, an initial condition of 0.4 was used because the slope consistently stabilized earlier for this initial condition than for others. The slope seems to slowly and smoothly change as r increases through the periodic regime. It changes more quickly and in a less smooth and regular way through the chaotic regime, though the behavior at the beginning of the chaotic regime looks very similar to the behavior for periodic r 's. It is thought that some of the peaks in the slope in the chaotic regime correspond to some underlying properties of the map. It should be noted that because of the computational nature, there may be more detail to how the slope changes with r that is too fine to be captured at this resolution. The dependence is seen in Figure 2.5.

2.3. CHAOTIC REGIME

It has been pointed out that the points in the periodic regime pair in a specific order. Similarly (and perhaps surprisingly) the points pair in a specific order in the chaotic regime as well. A local max is almost always paired with the following point in the iteration, which happens to be a local minimum. An instance of this failing to be true has not been observed. In fact, in the chaotic regime, it is postulated that the intermediate points, which are neither a local maximum nor a local minimum (and thus are not candidates to be paired for the persistence diagram) always precede a maximum, so they do not affect this pairing pattern.

One might expect the slope of the line formed in the persistence to vary as r is varied. In fact it does, but not greatly. Regardless of the initial condition in the chaotic regime, this slope remains between -0.3 and -0.42 . (There are usually a few points that don't fall on the line created by the rest of the persistence points. This will change with initial condition and slightly change the slope. The effect is smaller the more points that are used to compute

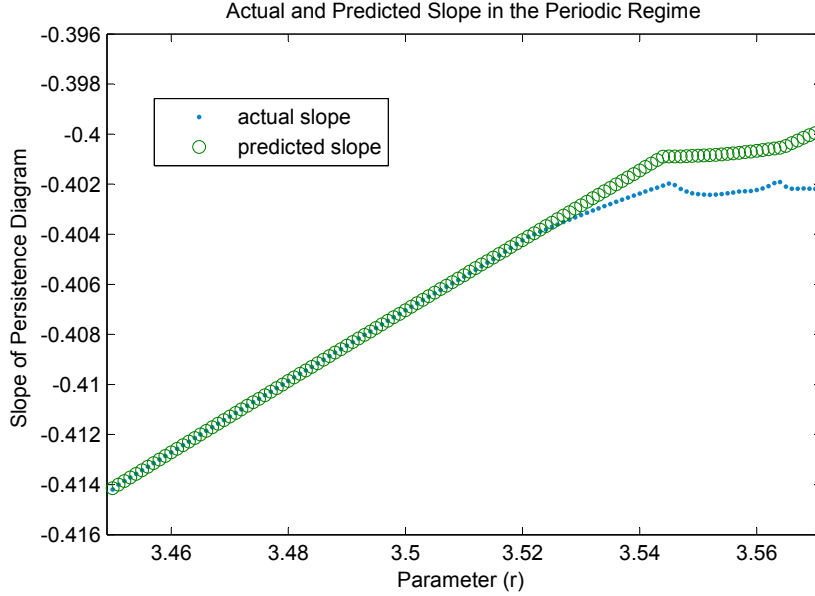


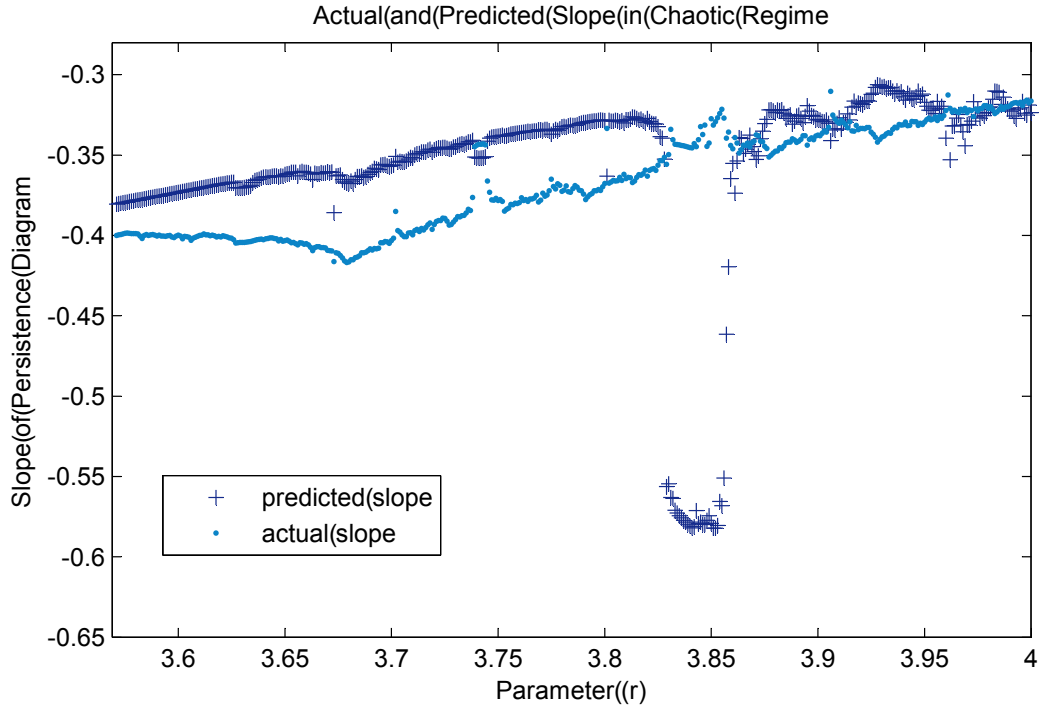
FIGURE 2.6. The actual slope and the slope calculated with the pairing function, using the value of the highest stable orbit.

the persistence. At the onset of chaos at $r \approx 3.569945$ the slope does not change much as r is increased.

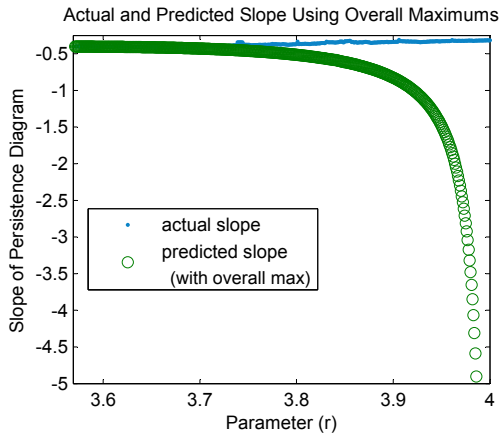
The observation of the order of pairing can be used to estimate the slope. Because of this order, the slope can be written in the following way:

$$\frac{f^2(x_n) - x_n}{f^3(x_n) - f(x_n)} = \frac{1}{(x_n - 1)(rx_n - 1)(-rx_n^2 + r^2x_n^2 + rx_n + 1)r}$$

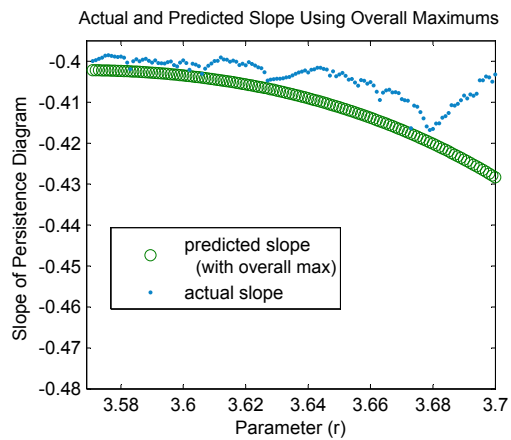
given that x_n is a local maximum. As expected, this works well in the periodic regime (since after stability is reached, there are no intermediate points). Figure 2.6 shows the very close correspondence through the periodic regime. As the period doubles, the actual slope and the estimate move slightly apart, but are still within ± 0.002 . In the chaotic regime, since this function depends on the value of the maximum, two methods were explored. First, the overall maximum from the first 10,000 iterations was used as the input. The results are seen in Figure 2.7b. Initially this seems to be a good choice, but as r increases, the predicted



(A) Actual and predicted slope of the persistence diagram using the average of all maximums occurring in 10,000 iterations. The period-3 window begins at $1 + 2\sqrt{2} = 3.82842\dots$

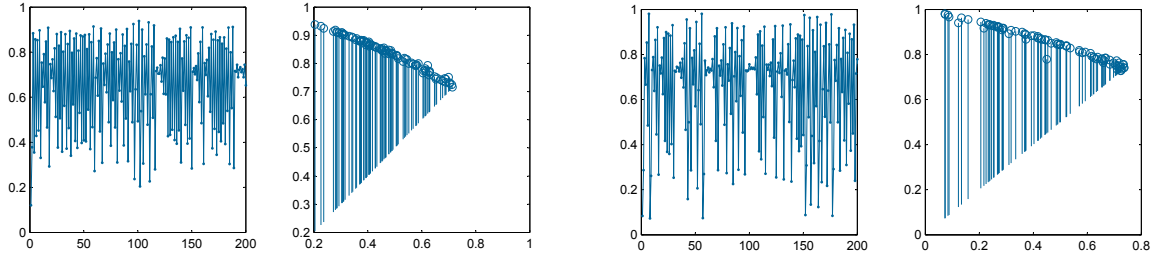


(B) The actual slope and the slope calculated with the pairing function, using the maximum orbit value in 10,000 iterations.



(C) A magnification of the beginning of the chaotic regime. The actual slope and the slope calculated with the pairing function, using the maximum orbit value in 10,000 iterations are shown. For this region this is a better estimate.

FIGURE 2.7



(A) Persistence for the logistic map (in the periodic regime) formed by drawing r from a Normal distribution centered around $r = 3.55$ and a standard deviation of 0.1

(B) Persistence for the logistic map (in the chaotic regime) formed by drawing r from a Normal distribution centered around $r = 3.8$ and a standard deviation of 0.1

FIGURE 2.8

slope quickly becomes far too steep. So local maximums were found from 10,000 iterations and averaged. This was checked across 50 different initial conditions and 20 r values in the chaotic regime and the value stabilized across all tested initial conditions for each r value. This value (for each r) was then used in the pairing function. As seen in Figure 2.7a, this estimate seems to at least to generally track the shape of the trend of the slope. The large dip in the predicted slope around 3.828 occurs during the 3-periodic window.

2.4. RANDOM OR STOCHASTIC r VALUES

To investigate further, the system was allowed to evolve in such a way that each r value was randomly selected from either two values for r that were within 0.1 of each other or from a Normal distribution about a particular r value with a standard deviation of 0.1. The results of the second method can be seen in Figure 2.8. The line in the persistence diagram still appears here, though it is a little more “fuzzy.” This means that this technique could prove to be useful in understanding dynamic structure of real data (which tends to be noisy).

CHAPTER 3

WHERE IS THIS PATTERN COMING FROM?

3.1. FEIGENBAUM'S SCALING CONSTANT

It seems somewhat remarkable that the points in the persistence diagram would lie nicely on a line in the periodic regime, even before the system has reached an equilibrium but what is more remarkable is that this pattern is still clearly visible in the chaotic regime, (though slightly bent downward in this regime). A clue to what is going on here may lie in a fundamental scaling constant α discovered by Mitchell Feigenbaum in 1978 [17] (much to his surprise) and later explicitly found [14] and proved by him in 1983 [18]. This is similar to Feigenbaum's constant δ discussed earlier, which applied to maps undergoing a period-doubling cascade to chaos. This next scaling constant applies to unimodal maps, which are maps of the form $x_{n+1} = \lambda f(x_n)$, scaled so that $0 < \lambda < 1$ and that satisfy the following conditions [18]:

- f is well-defined, continuous, piece-wise C^1 , and has a unique differentiable maximum occurring at $\bar{x} \in [0, 1]$. (Feigenbaum scaled such a function so that $f(\bar{x}) = 1$)
- $f(x) > 0$ on $[0, 1]$ and zero at the endpoints. f is strictly increasing on $(0, \bar{x})$ and decreasing on $(\bar{x}, 1)$
- For some $\Lambda < \lambda < 1$, $\lambda f(x)$ has two fixed points that are both repelling fixed points
- In the neighborhood about \bar{x} , $|f''(x)| < 1$, that is f is concave down.

For maps that meet the above conditions, which are remarkably nonrestrictive, Feigenbaum was able to discover α and δ , two profound quantitative constants of unimodal maps, regardless of the exact form of f ! This is an example of dynamic universality in these iterated

maps. That is, even though these maps have a different form, dynamically they behave in a way that is not only qualitatively similar, but quantitatively similar! In this context we are most interested in the scaling factor α . We will focus specifically on how it appears in the logistic map. One should note that the logistic map does indeed meet all of the listed criteria except that the parameter, r , corresponding to λ above does not fall between 0 and 1. With a simple re-scaling, ($\lambda = \frac{r}{4}$) all of the theory still applies and so this becomes a matter of convention. We will, through the course of the discussion, continue to use $0 < r < 4$.

In [18] Feigenbaum defines α in the following way. For each periodic cycle, we can find a unique value of r for which 0.5 is a fixed point. We may do so relying on Newton's method to solve $f^{2^n}(r, 0.5) = 0.5$ for r . It was necessary to use an informed starting point for r , estimating from the bifurcation diagram for stability of Newton's method. When these r values were used in the iteration of the logistic map with a starting value of 0.5, if there were no numerical approximation error, 0.5 would be a fixed point. However it was found that these parameters produced a fixed point at 0.5 ± 0.000001 . This was considered sufficient for this investigation. Collect such values of r in a sequence, $\{\lambda_1, \lambda_2, \lambda_3, \dots\}$ where λ_n is the parameter value for which 0.5 is a fixed point of the 2^n -cycle. The calculated values for these parameters are shown in Table 3.1.

Define d_n as the distance from $x = 0.5$ to the nearest fixed point in the stable periodic cycle for parameter value λ_n . Note that this will occur on alternating sides of $x = 0.5$ from one stable periodic orbit to the next. On the bifurcation diagram (Figure 3.1) the horizontal line is at $x = 0.5$ and the first several d 's are labeled. They quickly become impossible to discern on the bifurcation diagram because their length is scaled down by α every time (and recall that the distance between period doubling bifurcations shrinks by Feigenbaum's

TABLE 3.1. Numerical approximations for first five parameters for the logistic map where Feigenbaum’s scaling occurs.

Parameter	Value
λ_2	$1 + \sqrt{5}$
λ_4	3.498561720357923147
λ_8	3.55464086306839
λ_{16}	3.56666748775647465
λ_{32}	3.56924467659

constant $\delta \approx 4.66$.) If we consider α to be positive, then $\frac{d_n}{d_{n+1}} \sim \alpha$. As n goes to infinity, this ratio converges to $2.50290787509957\dots$ [18]. This means that the distance between $x = 0.5$ and the next nearest fixed point shrinks by approximately α for each successive λ_n . Actually, α is negative. This will be discussed briefly.

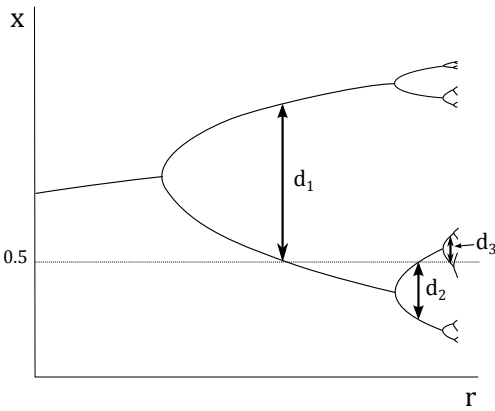


FIGURE 3.1. The width of the tines of the branches is scaled down by a factor of approximately α with each successive period doubling.

The graph of the logistic map lends itself in an alternate way to visualize α . Recall that fixed points occur at the intersection of the function and the bisectrix, (given that the magnitude of the slope of the graph at that point is less than one). Likewise, to visualize the orbit of a 2^n -periodic cycle, we consider where the graph of f^{2^n} intersects the bisectrix. Consider the graph of $f^{2^n}(x)$ depending on the parameter λ_n . Recall that for λ_n , $x = 0.5$ is a fixed point. If we draw a box with one corner at $(0.5, 0.5)$

and the opposite corner at the intersection of the nearest fixed point and the bisectrix, this is a square with side length d_n . In Figure 3.2, this is the shaded box for the 2-cycle, 4-cycle

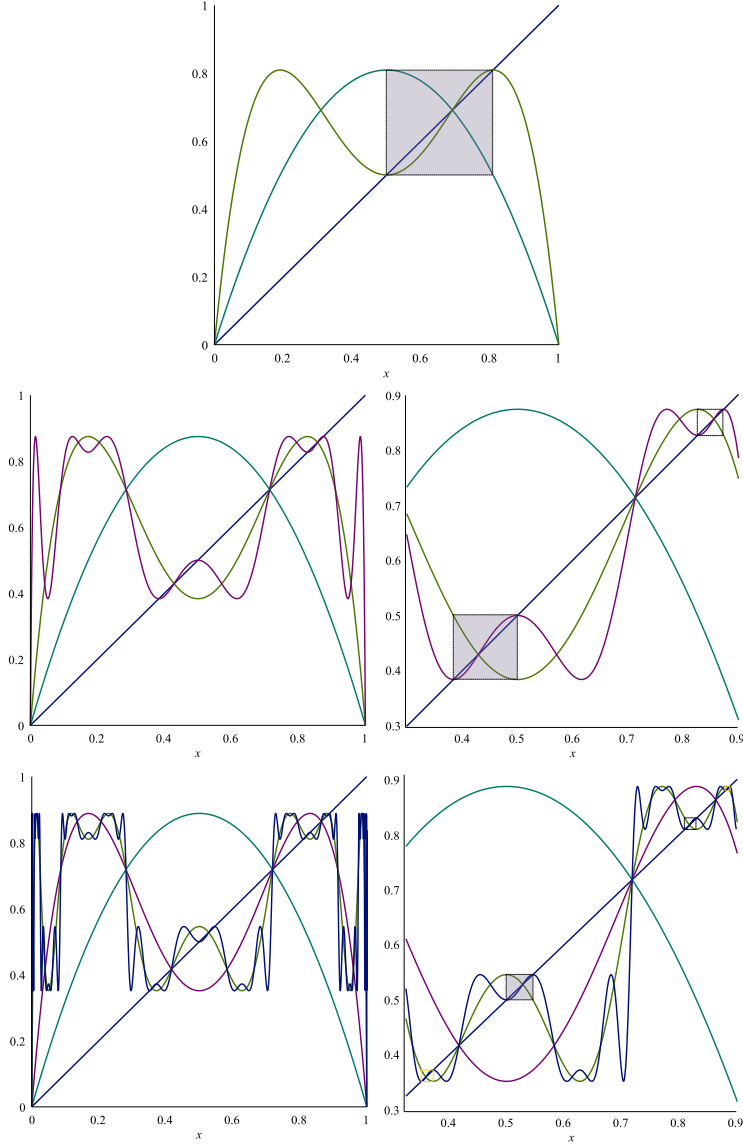


FIGURE 3.2. The first several boxes shown on plots of iterations of f at λ_1 , λ_2 and λ_3 respectively. The shaded box in the center shrinks by approximately α in each following step.

and 8-cycle. We can add a second box on the graph of the 4-cycle in a similar fashion, where the corners are fixed points.

When scaled appropriately by α the section of f that falls within the shaded box shown above with one corner at $(0.5, 0.5)$ and the opposite corner at the nearest fixed point, in the limit, will approach a specific function [18]. Notice that the function inside this box flips for

every λ_n . This is where the negative sign of α comes into play. New “boxes” are formed after every period doubling bifurcation. These occur in the same manner: as r is increased the slope of f at a fixed point will grow until the slope reaches a magnitude of one and then will exceed one and two new fixed points will be formed. The progression is schematically shown in Figure 3.3.



FIGURE 3.3. The progression of period doubling and the formation of two new fixed points. The intersection in the center is not a fixed point since $|f'(x)| > 1$ which causes the point to be unstable.

We are now set to relate this to the slope in the persistence diagram. We will begin with the stable period-4 case. In this case, there are two local maximums and two local minimums and therefore the persistence diagram will

have only two bars as seen in Figure 3.4.

When computing the slope of the persistence diagram, this is the ratio of the distance between maximums over the distance between

minimums of the orbit. For the persistence diagram shown here, the slope is approximately -0.4070. In the period 4 case, this is

the ratio of the side length of the upper box with the side length of the lower box. It should be noted that $\frac{-1}{\alpha} \approx -0.39953$.

It has been seen previously that the maximums and minimums seem to always pair in a specific order. Any given maximum will pair with the point in the orbit immediately

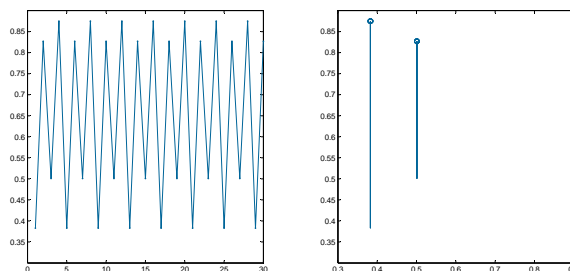


FIGURE 3.4. Shown on the left are 35 iterates of the logistic map in a stable 4-cycle with $r = 3.5$ and on the right is the associated persistence diagram.

following it, this will be a minimum. Also, the highest maximum pairs with the lowest minimum, the next highest maximum pairs with the next lowest minimum. The patterns continues until the smallest maximum is paired with the largest minimum. The slope then is the ratio of the side lengths of a box formed between maximum values and a box formed between minimum values. Care must be taken, however, to compare the correct boxes: the highest one and lowest one, the second highest and second lowest and so on.

Transitioning from a 4-periodic orbit to an 8-periodic orbit, we know that for a specific r value, the boxes appearing in the diagram of the updating function for the 4-cycle will be scaled by approximately alpha and two new ones will appear. (We say approximately because α holds in the limit, and we are considering the first several ratios in this limit.) This in fact holds for more boxes! As the period doubles, the fixed point at the corner of each box will bifurcate a new box can be formed with these two new points. One box will become two boxes at the next λ_n . One of these boxes will have a side length of approximately $\frac{1}{\alpha}$ of the side length of the original box. An interesting pattern arises when we consider which of the two new boxes is the one scaled by α !

For these specific parameter values, the scaling of these boxes is shown in Figure 3.5 by the bold teal arrows. Beginning at λ_2 , the two boxes split into four (at λ_4) and the inner two boxes of the four new ones are the boxes that are scaled by α . Going from λ_4 to λ_8 , for every pair of boxes that bifurcates into four boxes, the outer two boxes of the four are scaled by α . Increasing the parameter to λ_{16} shows that the inner two boxes of every four are the boxes that are scaled. This pattern continues, alternating between inner pair and outer pair of four new boxes every time the parameter increases to the next λ_i . This creates a fractal-like pattern and is symmetric about 0.5 past the 2-cycle. If we think of the slope

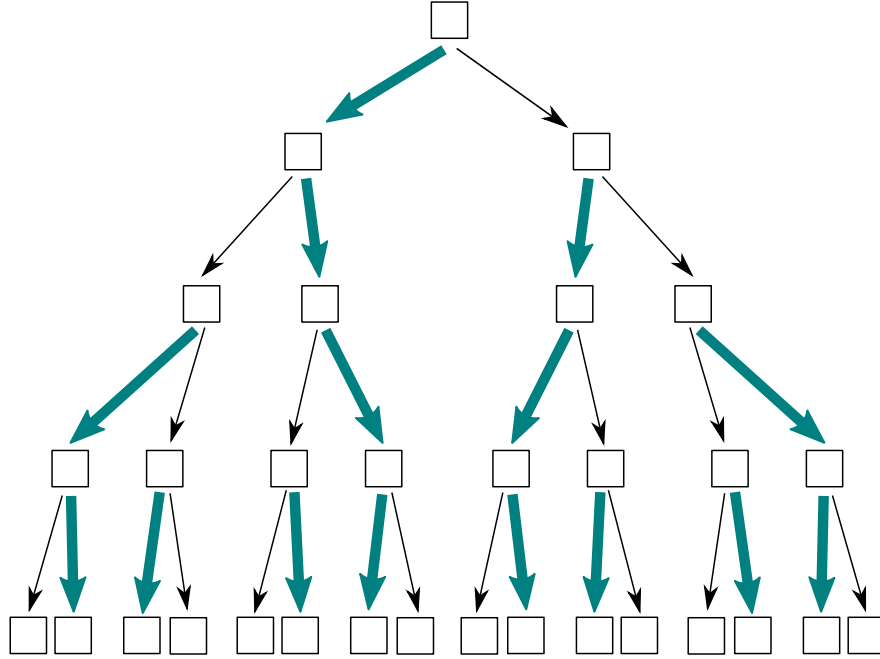


FIGURE 3.5. The bold teal arrows show (schematically) which boxes are scaled at the next λ_n .

of the persistence diagram as the ratio of side lengths of the boxes (keeping in mind that the correct boxes must be compared: the highest and lowest, the next highest and next lowest, and so on) then the symmetry in the way that these boxes scale gives a good indication why the slope should not change much in the periodic regime. When paired correctly, half of the new pairs will have the same ratio as the previous pairs because both the upper and lower boxes are $\frac{1}{\alpha}$

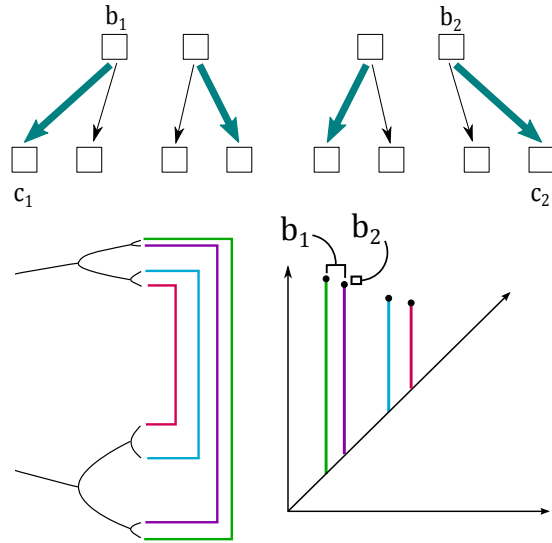


FIGURE 3.6. The schematic of α -box scaling, the bifurcation diagram, persistence diagram with the side lengths of two boxes shown.

the size of their original boxes! Focusing for a moment on the transition between λ_4 and λ_8 ,

Figure 3.6 clearly shows the correspondence between the side lengths of the boxes, the width of tines in the bifurcation diagram and the slope in the persistence diagram. Following the notation in the figure, the slope of the persistence diagram for λ_4 is given by the ratio of the side lengths of the boxes: $\approx \frac{b_2}{b_1}$. The slope of the persistence diagram for λ_8 is given by $\approx \frac{c_2}{c_1} \approx \frac{\frac{b_2}{\alpha}}{\frac{b_1}{\alpha}} = \frac{b_2}{b_1}$ when we take into account the α scaling. Therefore, this scaling constant at least indicates why the slope does not drastically change in the periodic regime. Recall that α is defined in the limit, so scaling by α is not exact in every step, and this gives some reason for the small fluctuation in slope as r increases through the periodic regime.

It seems that this scaling constant would dictate the actual slope of the persistence diagram, and at first seemed promising that for the logistic map, the slope was close to $\frac{1}{\alpha}$. However, this does not appear to be the case. α relates the width of “tines” of the bifurcation diagram at very specific parameter values. As r increases from one λ_i to the next, λ_{i+1} (as seen above) the factor of α cancels. The slope of the persistence diagram relates these widths of “tines” at a single parameter value, not across several parameters.

Further, since α is a universal constant for unimodal maps, then it should be the case that the slope of a line in the persistence diagrams for these maps is approximately $\frac{1}{\alpha}$ as well. The quadratic map, given by $x_{n+1} = x_n^2 + c$, which is topologically conjugate to the logistic map via a change of variables is qualitatively the same system. Conjugacy preserves invariants [16], and α is an invariant for these types of maps [18], so if the value of the slope is given by approximately $\frac{1}{\alpha}$ it should be the case for the quadratic map as well. The persistence diagram of the quadratic map does in fact display the same linear pattern in the persistence diagram, but the slope is different. This means the value of the slope is not so clearly connected to this scaling factor for all quadratic maps.

3.1.1. PERIODIC BEHAVIOR IN THE CHAOTIC REGIME. This give us occasion to explore some other features of the logistic map and consider their role in the creation of this slope. Recall that the periodic cycles exist as unstable cycles after period doubling occurs, and after r increases past

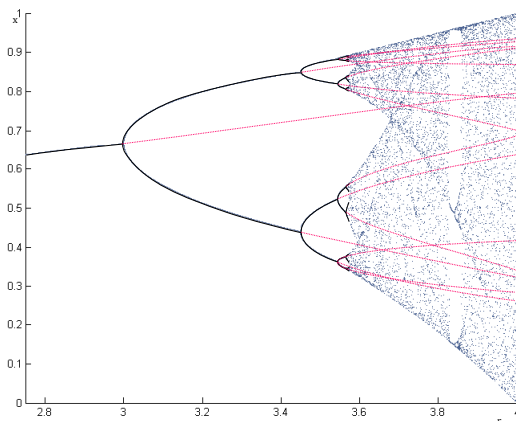


FIGURE 3.7. Bifurcation diagram with unstable orbits shown in magenta.

r_∞ . The unstable periodic cycles are dense in the chaotic regime. Figure 3.7 shows some

of the unstable cycles that carry into the chaotic regime. These unstable cycles are dense [13]. Thus if we start with any point in the, we will be close to some unstable periodic orbit for a few iterations (though the Lyapunov exponent indicated that we move away at an exponential rate, so this only holds for a few iterations). When we move away from this periodic orbit, we will be “close” to another periodic orbit for a few more iterations. In this

way, we are always “close” to some periodic orbit (albeit unstable) and thus the slope of the persistence diagram follows the same pattern. Also, periodic cycles are dense in the region $r > r_\infty$ so there are infinitely many r values for which the orbit is periodic and the pairing of points in the persistence diagram follows a similar pairing as discussed previously (though not precisely the same if the cycle is k -periodic for k odd). This means that remnants of periodic behavior could be driving the slope in the chaotic regime.

There is an interesting connection with the Lyapunov exponents and the slope of the persistence. Peaks in the slope often correspond to a periodic window, as seen in Figure 3.8. The large peak in the slope around 3.8284 is the large period-3 window. It should be

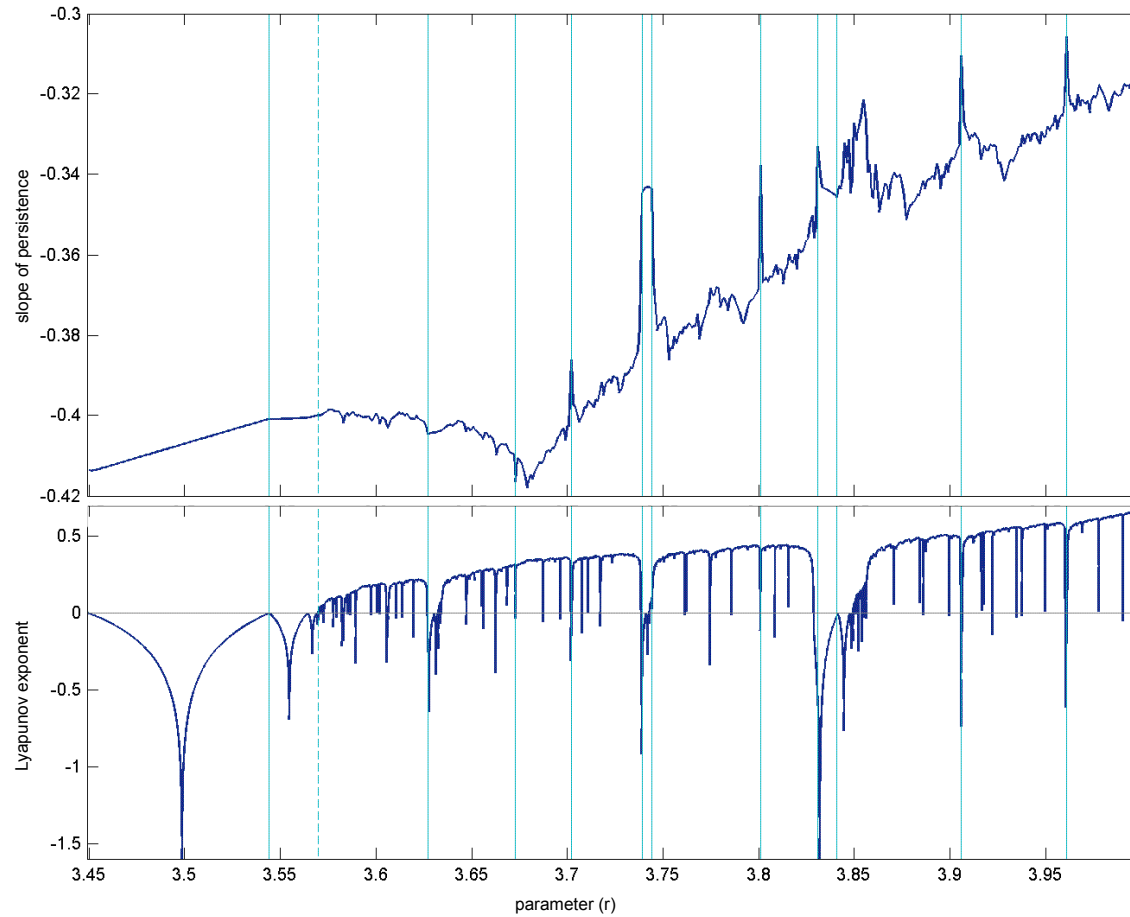


FIGURE 3.8. Comparison of the Lyapunov exponents and the slope of the persistence.

noted in this figure that there are infinitely many periodic cycles in the chaotic regime, but the Lyapunov exponent was calculated by incrementing r by 0.0001 so much of the periodic behavior is not visible.

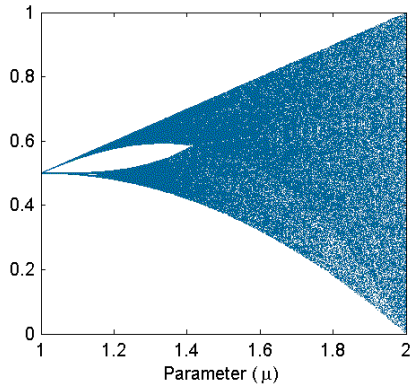
3.2. OTHER MAPS

The line in the persistence diagram in fact appears for other maps as well. Another common one dimensional map is the tent map, given by

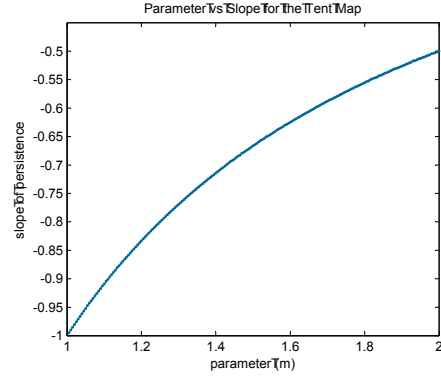
$$x_{n+1} = \mu \min(x_n, 1 - x_n)$$

is topologically conjugate to the logistic map, meaning that there is a homomorphism that can conjugate one map into the other. The homomorphism is given by $h(x) = \sin^2(\frac{\pi}{2}x)$ So that if $T(x)$ is the tent map and $L(x)$ is the logistic map, $L(x) = h \circ T \circ h^{-1}(x)$ [15]. This means that these maps behave the same dynamically [13], so quantitatively these maps may be different, however qualitatively the two maps display the same behavior.

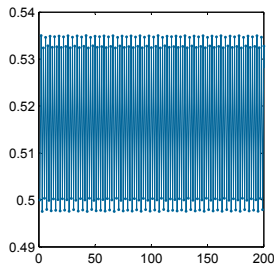
Stable orbits undergo a period doubling bifurcation that, like the logistic map, cascade to chaos as revealed in the bifurcation diagram of the tent map, Figure 3.9a. At any given parameter for the logistic map, the tent map at the conjugate parameter has the same number of unstable periodic orbits [16]. Further, Feigenbaum's scaling by δ and α still appear. The tent map is not technically considered a unimodal map because the maximum is not differentiable, however since this is a single point (a set of measure zero) it does not effect the dynamics. As seen in Figure 3.9, there is a clear, decreasing line in the persistence diagram both in the periodic and chaotic regime. Interestingly, as μ the slope of the persistence increases in a nice, smooth curve (see Figure 3.9b). Stability of the persistence diagram seems to be reached very quickly in this case.



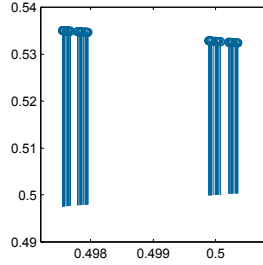
(A) Bifurcation of the tent map.



(B) Slope of the persistence diagram for the tent map as the parameter is varied.



(C) The persistence diagram for the tent map, $\mu = 1.07$



(D) The persistence diagram for the tent map, $\mu = 1.7$

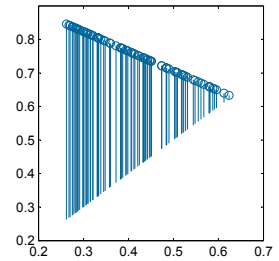
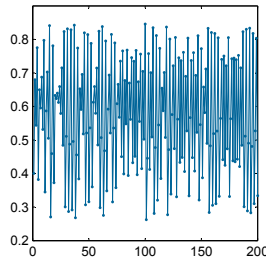
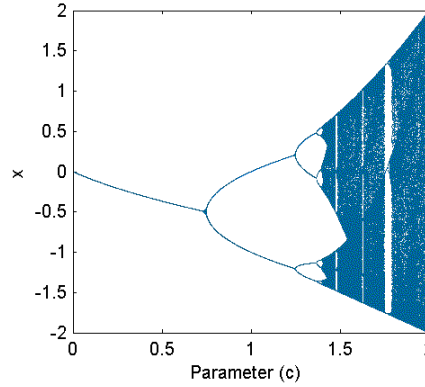


FIGURE 3.9

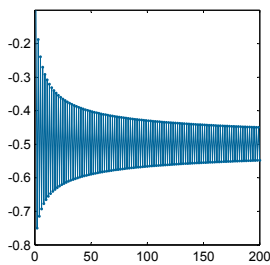
Another common conjugate of the logistic map is the quadratic map given by

$$x_{n+1} = x_n^2 + c$$

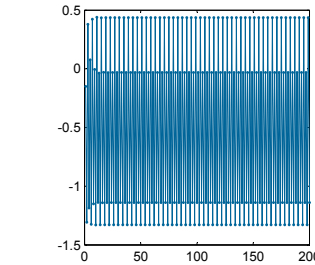
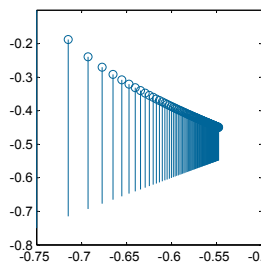
for $0 < c < 2$. As seen in Figure 3.10, the quadratic map displays the same dynamics as the tent and logistic map, however the line in the persistence diagram is a little more visibly curved than in other maps, and is curved in the opposite direction than the logistic map. The bifurcation diagram for the quadratic map appears qualitatively identical to the bifurcation diagram of the logistic map. The sine map, given by $x_{n+1} = \sin(\lambda\pi x_n)$ is also topologically conjugate to the logistic map for $0 < \lambda < 1$ and displays similar behavior as does the Gaussian map or Mouse map given by $x_{n+1} = e^{-\alpha x_n^2} + \beta$.



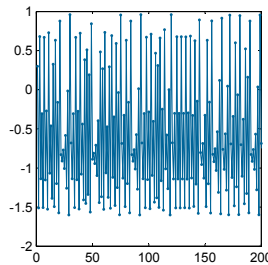
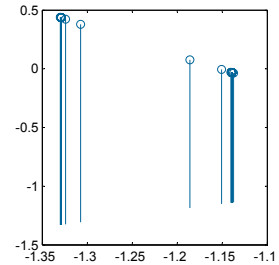
(A) Bifurcation of the quadratic map.



(B) Persistence diagram for the quadratic map, $c = 0.75$



(C) Persistence diagram for the quadratic map, $c = 1.33$



(D) Persistence diagram for the quadratic map, $c = 1.6$

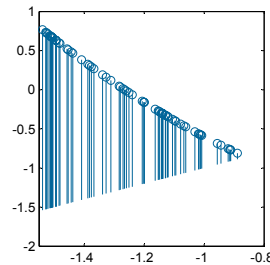


FIGURE 3.10

It should be noted that not all one dimensional iterated maps display this specific pattern in their persistence diagrams. For example, circle maps given by $x_{n+1} = x_n + \alpha \pmod{1}$ where α is the rotation number do not display a clear decreasing line in the persistence diagram. If $\alpha = \frac{1+\sqrt{5}}{2}$ (the Golden ratio) then the persistence diagram displays sets of points that line up in an increasing line (in Figure 3.11), with the number of these sets increasing as the number of iterations increases. In fact, as the number of iterations increases, the number of these

lines will increase when the number of iterations reaches a Fibonacci number! However, there seems to be no generalized pattern that appears for a general α . Rational and irrational rotation numbers will display different behaviors, but even when restricting α in such a way, there is not a clear general pattern.

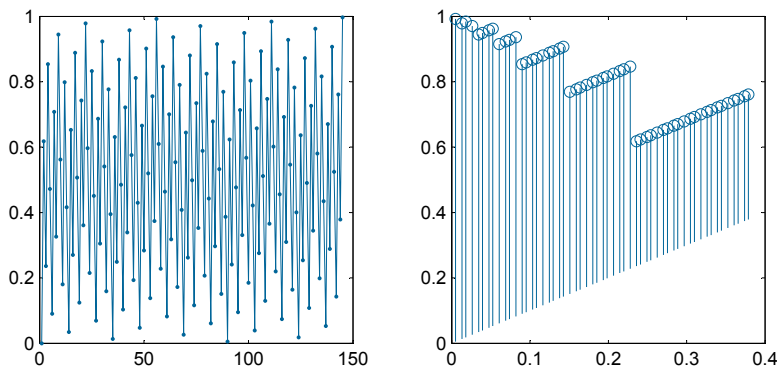
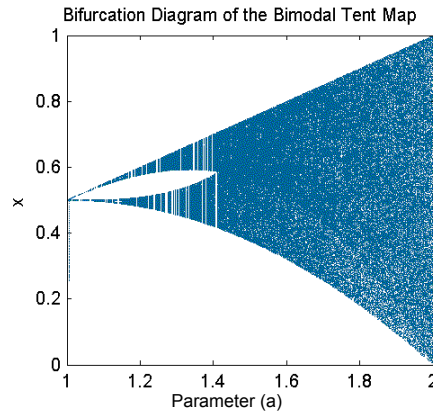
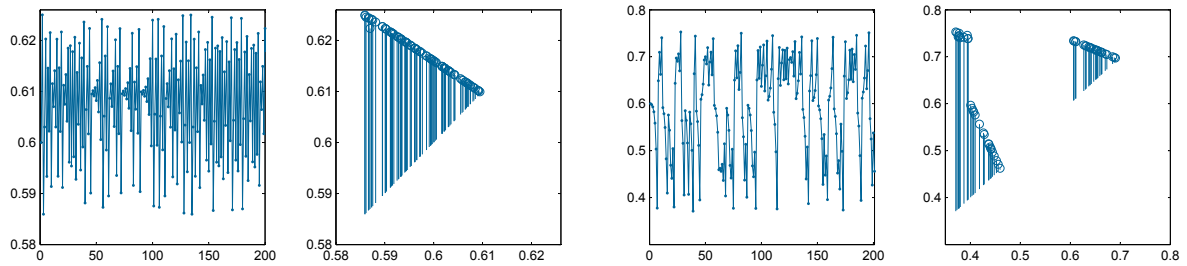


FIGURE 3.11. Persistence diagram of the circle map with $\alpha = \frac{1+\sqrt{5}}{2}$ (the Golden ratio) as the rotation number.

The bimodal tent map is another iterated map for which the persistence diagram displays interesting behavior. For parameter values $\mu < \sqrt{2}$ There is a clear line in the persistence diagram (see Figure 3.12b), but if one closely examines the bifurcation diagram in Figure 3.12a, it seems that the orbit will remain on either the top or bottom “tine” (this actually depends on the initial condition.) From the perspective of cobwebbing, the orbit remains under one peak of the bimodal map and so it acts like the tent map in these regions as seen in Figure 3.12b. However, once $\mu > \sqrt{2}$, the shape of the persistence diagram changes as seen in Figure 3.12c and three distinct regions emerge. There are two lines that seem to correspond to the two peaks in the bimodal map, and there are points that form a small cloud in the upper left of the persistence diagram. This pattern remains as μ is increased.



(A) Bifurcation of the bimodal tent map.



(B) Persistence diagram for the bimodal tent map, $\mu = 1.2$

(C) Persistence diagram for the bimodal tent map, $\mu = 1.51$

FIGURE 3.12

3.3. GENERALIZATION

The persistence diagram has been computed for many different sets of data arising from many different maps. When the map is unimodal, a nice line appears in the persistence diagram. This leads to the following conjecture:

CONJECTURE: A decreasing line will appear in the persistence diagram of any one dimensional unimodal map.

A sketch of the proof and a discussion of difficulties that arise is offered. All unimodal maps have the same qualitative behavior as a dynamical system [17]. This means that they will undergo a period doubling bifurcation cascading to a chaotic regime as the parameter is increased. Justification for the appearance of the slope in the periodic regime follows from

the α -box scaling that occurs as the period doubles. Because α is a universal scaling constant for all unimodal maps the previous discussion on its connection to the slope of the persistence diagram for a stable periodic orbit holds here. This accounts for a fairly consistent slope across very specific parameters, however the pattern appears across all parameters. The argument should be extended, possibly through continuity, to these parameters. Further, is not well understood why the transient behavior almost always falls along this line as well.

In the chaotic regime, as discussed earlier, since periodic orbits are dense in the chaotic regime a point is always “close” to an unstable periodic cycle for a few iterations. The rate at which trajectories of points that are initially very near to each other depends on the Lyapunov exponent for that specific parameter. Currently the Lyapunov exponent is calculated numerically, but will need to be computed analytically for use in a proof. It is thought that the ghost of periodic behavior is appearing in the persistence diagram in the chaotic regime.

Apart from the line itself appearing, it is not yet understood what causes the value of the slope itself. It is known that the value of the slope is not universal, for if it were, there would be no difference across different maps. There is, however, a difference. As a last remark, the “line” that appears is indeed a clear pattern, however it is not perfectly linear. It is slightly concave down for the logistic map and slightly concave up for the quadratic map. The pattern is striking, but the statement of the conjecture needs to be made precise. The clearest and most stable line in the persistence diagram appears for the tent map. Continuing work will be done on this proof.

3.4. EXTENDING TO HIGHER DIMENSIONS

The clear line in the persistence diagram is also seen in continuous ordinary differential equations in higher dimensions like the Rössler attractor and the Lorenz system! The Lorenz system, given by

$$\dot{x} = \sigma(y - x)$$

$$\dot{y} = rx - y - xz$$

$$\dot{z} = xy - bz$$

(where the dot indicates the time derivative) is a classic example of deterministic chaos [12]. Lorenz was able to construct an approximate one dimensional map from this system by plotting successive maximums [19, 20]. When this is done for the z variable, this gives rise to a single peaked map. Lorenz was able to use this to convincingly argue that the system was chaotic [15]. This is exciting because it is precisely in the variable z in the persistence diagram that we see the clear decreasing slope! (see Figure 3.13) In general, if the Lorenz map of a system is nearly unimodal, much of the universality theory applies [21].

The Rössler system, given by

$$\dot{x} = -y - z$$

$$\dot{y} = x + ay$$

$$\dot{z} = b + z(x - c)$$

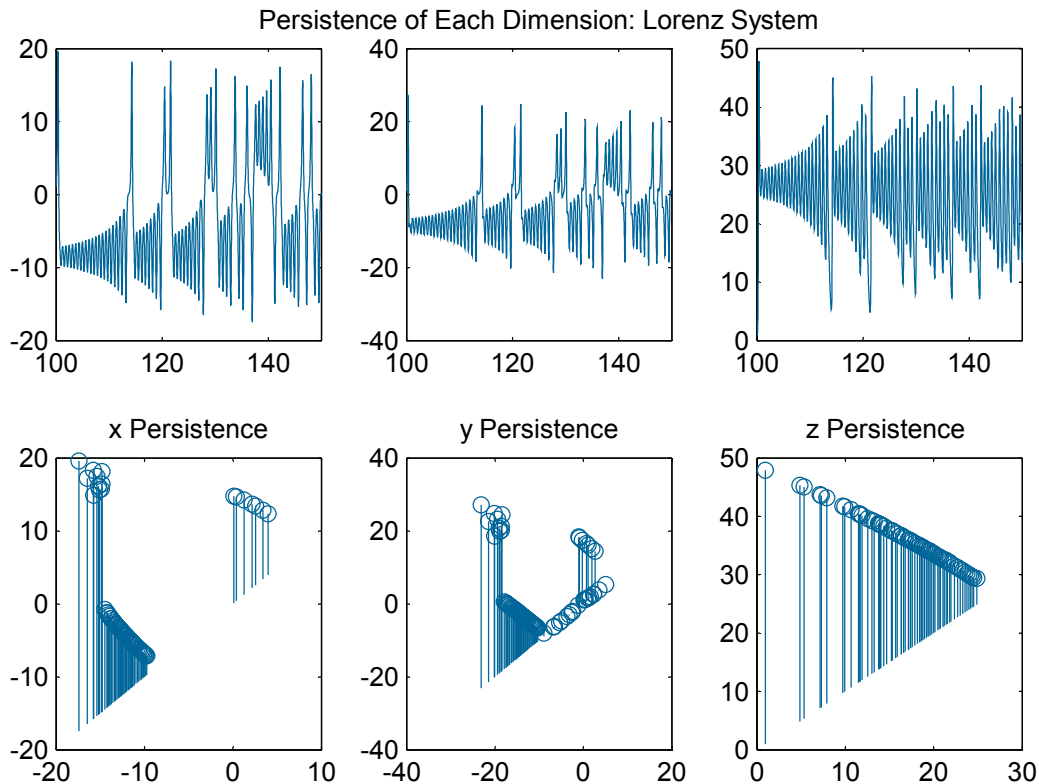
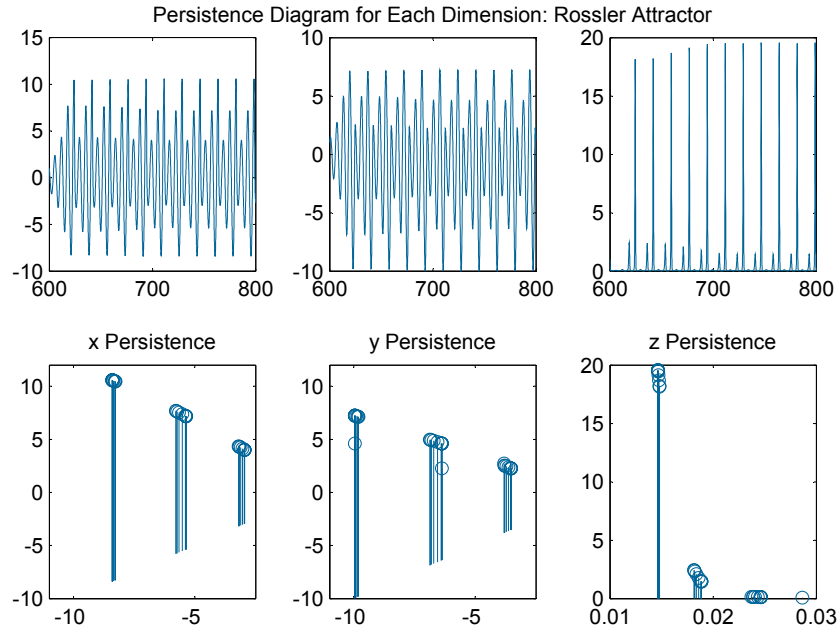
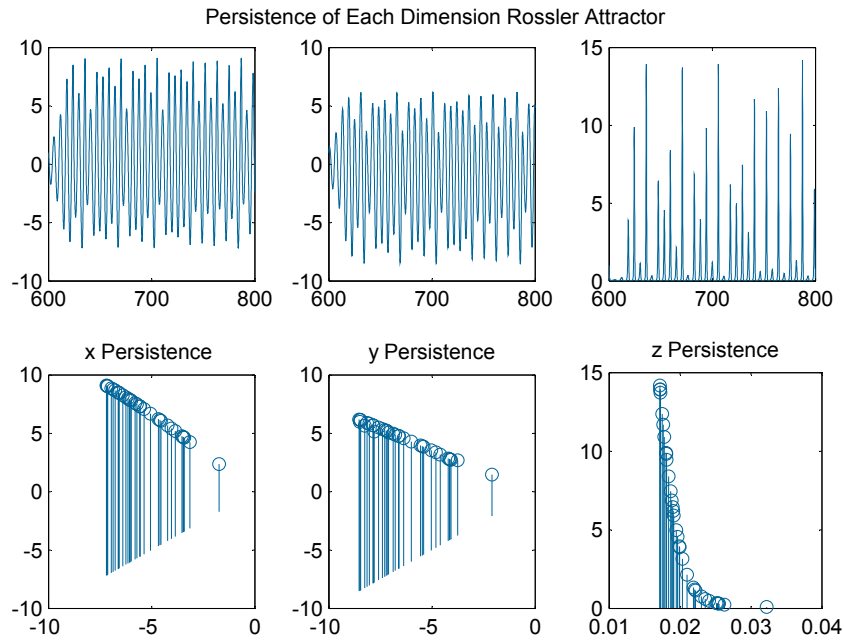


FIGURE 3.13. The persistence diagram for each variable of the Lorenz system with $\sigma = 10, b = \frac{8}{3}, r = 28$, parameters at which the system is a strange attractor.

contains several of the familiar features of the logistic map. If we let $a = b = 0.2$ and let c vary, projecting the attractor's behavior into the xy plane allows us to see a single limit cycle for $c = 2.5$ as c increases, the limit cycle must go around twice to close, then 4 times, etc. This is in fact period doubling in a continuous system. After the infinite cascade of period doubling, chaos arises. In this case it is referred to as a strange attractor (with a few more technical details added to our previous understanding of chaos). This map cannot be reduced to something as simple as the logistic map, however plotting successive maximums for the x variable will give rise to a single hump, which indicates deterministic chaos in the system. The same can be seen in the y variable [22]. This means that underneath the continuous



(A) Persistence diagram for each variable of the Rössler attractor. $a = b = 0.2, c = 5.26$.



(B) Persistence diagram for each variable of the Rössler attractor. $a = b = 0.2, c = 4.5$

FIGURE 3.14

system, there is a simple one dimensional map, which is unimodal [21]. In fact, if we restrict our attention to the trajectory of this map in a single variable, and look at the persistence

diagram, we can see the same decreasing linear pattern for both the x and y variables! Figure 3.14b shows the persistence broken down for each variable. The persistence diagram clearly shows the one dimensional deterministic chaos that is the backbone of this system. The top example is a periodic limit cycle and the second example is a strange attractor.

We were able to apply the theory of universality to both of these maps, but it should be noted that this requires the system to be highly dissipative, that is, there are only a few degrees of freedom that are active, the others follow passively [22].

CHAPTER 4

CONCLUSIONS

The appearance of a clear pattern in the persistence diagram for both the periodic and chaotic regime of the logistic map is unexpected. While it is not surprising that this pattern appears in the stable regime, it is quite surprising that the transient behavior at the beginning conforms to this pattern as well. What is even more remarkable is the clarity and consistency of this pattern in the chaotic regime regardless of the initial condition. In the chaotic regime a tiny change in the initial condition grows exponentially as the orbit is traced, a feature of chaos that can make it difficult to study. The pattern in the persistence diagram stabilizes in the chaotic regime regardless of initial condition! It is thought that the density of unstable periodic orbits in the chaotic regime lends a clue as to why this behavior might arise.

This pattern in the persistence diagram is not exclusive to the logistic map. It is hypothesized that this clear pattern appears in the persistence diagram for any unimodal map, regardless of the parameters or whether or not the behavior is chaotic. It is interesting that even though the quantitative slope changes, the qualitative pattern remains even though the orbits of points changes dramatically as r is increased or as the form of the map is changed. The conjecture is compelling, though stands to be made precise and proven rigorously.

The clear line in the persistence diagram even appears in single variables of three dimensional ODE's that have a unimodal map (or two) as a backbone. This is a new way to detect this type of structure in an ODE system. This method gives rise to clear patterns in systems of deterministic chaos, which could be used in applications to understand governing systems of sets of data. This could prove to be more useful than the peak-to-peak method

used commonly (first by Lorenz [19]) to uncover a governing map from the set of points in a chaotic orbit because a few missing points will have a smaller overall effect.

Persistent homology is a novel and powerful tool to study and hopefully better understand discrete time dynamical systems and ordinary differential equations. It could give us a better way to discuss and compare topological features of a dynamical system. Persistent homology seems to be able to pull out some deep qualitative behavior of the system, in this case, deterministic chaos.

Persistent homology has a history of applications to a wide variety of problems, using simplicial homology to better understand complex networks [3] to the structure of stories [4]. Persistent homology is particularly useful for real data sets because of its ability to classify and see past noise and sampling distortion in a system, highlighting the more prominent features. Beyond this project, persistent homology is yet to be studied as a tool to understand dynamics. This area is rich and there are many avenues yet to be walked down. The persistence allows us to “see” sets of data in a unconventional way. There is much to be explored here!

BIBLIOGRAPHY

- [1] W. Commons, “File:seurat-la parade detail.jpg.” en.wikipedia.org/wiki/File:Seurat-La_Parade_detail.jpg#globalusage.
- [2] G. Carlsson, “Topology and data,” *American Mathematical Society*, vol. 46, pp. 255–308, 2009.
- [3] D. Horak and Maletić, “Persistent homology of complex networks,” *Journal of Statistical Mechanics*, no. P03034, 2009.
- [4] X. Zhu, “Persistent homology: An introduction and a new text representation for natural language processing,” in *IJCAI 2013, Proceedings of the 23rd International Joint Conference on Artificial Intelligence, Beijing, China, August 3-9, 2013*.
- [5] K. G. Wang, “The basic theory of persistent homology,” 2012. REU participating paper.
- [6] H. Edelsbrunner, D. Letscher, and A. Zomorodian, “Topological persistence and simplification,” *Foundations of Computer Science, 2000. Proceedings. 41st Annual Symposium on.*, pp. 454–463, 2000.
- [7] H. Edelsbrunner and J. Harer, “Persistent homology — a survey,” *In Twenty Years After*, eds. J. E. Goodman, J. Pach and R. Pollack, AMS., 2007.
- [8] S. Weinberger, “What is persistent homology?,” *Notices of the AMS*, vol. 58, no. 1, pp. 36–39, 2011.
- [9] H. Edelsbrunner and J. Harer, *Computational Topology, An Introduction*. American Mathematical Society, 2010.
- [10] M. Vejdemo-Johansson, “Sketches of a platypus: Persistent homology and its algebraic foundations,” *ArXiv e-prints*, 2012.

- [11] S. H. Strogatz, *Nonlinear Dynamics and Chaos: With Applications to Physics, Biology, Chemistry and Engineering*. Addison-Wesley Publishing Company, 1994.
- [12] M. W. Hirsch, S. Smale, and R. L. Devaney, *Differential Equations, Dynamical Systems and An Introduction to Chaos*. Elsevier, second ed., 2009.
- [13] R. Gilmore and M. Lefranc, *The Topology of Chaos: Alice in Stretch and Squeezeland*. Wiley, second ed., 2012.
- [14] M. J. Feigenbaum, “Quantitative universality for a class of nonlinear transformations,” *Journal of Statistical Physics*, vol. 19, no. 1, pp. 25–52, 1978.
- [15] J. D. Meiss, *Discrete Dynamical Systems*. 2014. in preparation.
- [16] E. Ott, *Chaos in Dynamical Systems*. Cambridge University Press, second ed., 2002.
- [17] M. J. Feigenbaum, “Universality in complex dynamical systems,” *Los Alamos Theoretical Division Annual Report*, pp. 98–102, July 1975–September 1976.
- [18] M. J. Feigenbaum, “Universal behavior in nonlinear systems,” *Physica D: Nonlinear Phenomena*, vol. 7, no. 13, pp. 16–39, 1983.
- [19] E. N. Lorenz, “Deterministic nonperiodic flow,” *Journal of the Atmospheric Sciences*, vol. 20, no. 2, pp. 130–141, 1963.
- [20] H. Fang, “Studying the lorenz equations with one-dimensional maps from successive local maxima in z,” *Zeitschrift fr Physik B Condensed Matter*, vol. 96, no. 4, pp. 547–552, 1995.
- [21] J. Yang, “Universality.” lecture notes, 2012. www.emba.uvm.edu/~jxyang/teaching/Math266notes7.pdf.
- [22] P. Bergé, Y. Pomeau, and C. Vidal, *Order Within Chaos: Towards a Deterministic Approach to Chaos*. Wiley, 1984.